International Journal of Robotics and Control Systems
Vol. 4, No. 3, 2024, pp. 1279-1303
ISSN 2775-2658
http://pubs2.ascee.org/index.php/ijrcs

Honey Badger Algorithm Based DVR Controllers for Improved Power Quality in a Microgrid Combined of (Wind System\ Grid\Nonlinear Load)

Ahmed Atef Zidan [a,1], Ahmed M. Ibrahim [a,2], Ahmed I. Omar [b,3,*]

[a] Electrical Power & Machines Engineering Department, Faculty of Engineering, Cairo University, Cairo 12613, Egypt
[b] Electrical Power and Machines Engineering Department, The Higher Institute of Engineering at El-Shorouk City, El-Shorouk Academy, Cairo 11837, Egypt
[1] Ahmed.201920011@eng-st.cu.edu.eg; [2] drahmedibr@gmail.com; [3] a.omar@sha.edu.eg
* Corresponding Author

ARTICLE INFO

Article history
Received May 26, 2024
Revised July 10, 2024
Accepted July 27, 2024

Keywords
Grid Faults;
Dynamic Voltage Regulator;
Control Strategy;
Honey Badger Optimizer;
Wind Energy

ABSTRACT

Power quality (PQ) is crucial in today's energy supply networks, where even little voltage fluctuations can have a big impact on how well household appliances and technologies operate. The suggested dynamic voltage regulator (DVR) approach helps to create a new generation power grid that is more dependable and effective. In this study, the honey badger optimizer (HBO) is used to optimize the controllers of the DVR for improving PQ via voltage control. The efficacy of the optimized DVR is further increased by its integration with a microgrid (MG) wind supply. The suggested technique makes use of a low-complexity control approach for voltage regulation to adjust for harmonic distortion, swells, and voltage dips in the addressed system. The technique accomplishes voltage improvement, bus stabilization, energy-efficient utilization, and harmonic distortion reduction by using the DVR in conjunction with an MG wind supply. Various voltage disturbances, such as balanced and unbalanced swell and sag, voltage imbalance, notching, various fault states, and power system harmonic distortion, are taken into consideration to show the approach's usefulness. The findings indicate PQ enhancement, demonstrating that the load voltage roughly matches the nominal value.

1. Introduction

Despite somewhat reliable electricity production today, power quality (PQ) problems still exist and present difficulties. These PQ issues are becoming a serious concern because of the increased demand for nonlinear loads in distribution lines [1]-[4]. The degree to which the real power supply and the theoretical power supply degree are indicated by the PQ. When the power grid's PQ is high, every load operates normally and to its maximum efficiency. Any additional demand placed on the network during a period of low PQ may cause equipment to malfunction or shorten its lifespan [5]-[7]. Electronic facilities have become pickier about the PQ in recent years. They want low harmonic distortion in the output voltage and unexpected voltage sags or surges. Unexpected voltage drops, primarily brought on by high-power motor starts or short circuits, are typically the most frequent interruptions to electrical systems. More than 90% of PQ problems are caused by them. Conversely, voltage swell occurs when high loads are removed, big-capacity devices are switched, and

unidirectional ground connection issues arise. Systems are greatly affected by sudden voltage sags [8], [9]. Voltage sag, swell, and flicker are just a few of the PQ challenges in the recent distribution system [9], [10]. One of the most difficult issues that industrial and commercial clients must deal with is voltage sag, which harms the performance of inductive motors, adjustable speed drives, process control systems, and computers. Sagging voltage is an important PQ problem that many industries and utilities contend with. It is the root reason for over eighty percent of the PQ troubles in power systems. the idiom "voltage sag" refers to a decrease in the AC voltage's RMS value. at power frequency that can last anywhere between a few seconds and a half cycle [11]-[13].

Robots, programmable logic controllers, adjustable speed drives, and process controls are examples of sensitive equipment used in modern industrial operations that cannot tolerate voltage sags. According to sources, voltage sags in industrial equipment like adjustable speed drives and programmable logic controllers are around 10%, while voltage sags in high-intensity discharge lamps used for industrial lighting are around 20% [14]-[17]. Dynamic voltage restorers (DVRs), which are used in distribution networks following IEEE 519 standards, protect loads against voltage-based PQ and important customer loads from loss and tripping [18]. On corrupted supply voltages, DVR can restore the load voltage to a sinusoidal voltage with the proper amplitude [19], [20]. As a result, by injecting a compensating voltage waveform into the distribution line, the DVR is modeled and controlled to perform a variety of functions [21]. DVR receives the compensating voltage. No active power is given to the DVR during an SSC [22].

In contrast, active power is required in capacitor-based DVR to compensate for VSC switching losses and regulate the DC link. DVR absorbs active power toward distributed systems according to the kind of load connected to the system to attain pre-sag voltage. Power device controls include instantaneous symmetrical components, current model control, p-q theory, and other processes that are investigated using various PI controllers. Various optimization techniques, such as NN, fuzzy logic, GA, and PSO, were examined in [23]-[25]. To switch VSC to the optimization strategy for generating reference voltage, use the control procedure. PI controllers are used to control DVRs [26], [27]. The DVR performance is dictated by the PI gain settings. Tuning parameters that are not always optimum producers. The primary PQ challenges are fluctuations, interruptions, flickers, harmonics, transients, voltage sags, and voltage swells. A recent study concluded that utilizing a DVR series compensator controlled by a PI controller with the GTA algorithm is an efficient approach for enhancing PQ issues related to RESs [28], [29]. Using DVR to enhance the electric voltage performance for sensitive loads, an improved management strategy was provided. The current control solutions either emphasize the best control through the steady-state stage of compensation or fix the phase angle jump during the first level of compensation. By safeguarding them during phase angle leaps with grid voltage sags, the adaptive methods enhance the voltage quality of sensitive loads. The DC link voltage is recovered and the phase shift in the energy self-recovery stage is also mitigated by the optimized energy self-recovery technique. In (Tu, 2019), the rational power transfer optimization (RETO) method was used to control the DVR in the distribution network since it is an efficient solution for voltage quality issues. The DVR converter successfully manages voltage and reactive power using the RETO-based inverter switching technology, decreasing grid losses while maintaining acceptable voltage levels. This optimization technology provides dynamic power control, which leads to large energy savings throughout the power distribution network. It also has a low total harmonic distortion (THD) of 5.67 percent. This implies that the algorithm effectively reduces harmonic distortions, resulting in a cleaner and more stable power supply. In addition, the proposed technique increases overall system efficiency by 92.63% [30]. In [31], it was proposed the efficacy of a suggested DVR-based technique for enhancing the harmonically distorted voltage. For blending 3^{rd} and 5^{th} harmonics, which are a power system model with a customizable power source was developed. It has been observed that the recommended DVR-based method effectively controlled the voltage distortion, resulting in a load voltage that has been smoothly corrected. With the insertion of the third and fifth harmonics in the supply voltage, the THD percentage of load voltage was roughly 18% and 23%, respectively. In both instances, the planned DVR's inclusion reduced THD by about 4% or less. In [32], was made an effort to mitigate and safeguard the effects

of grid-connected hybrid PV-wind power system voltage fluctuations. To achieve this, a DVR powered by batteries and supermagnetic energy storage (SMES) was employed as a compensating mechanism in the event of a voltage sag condition. Several voltage sag depths for asymmetrical and symmetrical voltage imbalance have been taken into account in the simulation, and the HES-based DVR performed effectively.

The voltage source converter (VSC) system and the DC-DC buck/boost converter of the battery were used to implement two different controlling stages for the suggested battery energy storage-based DVR. The battery's state of charge (SOC) value and the measured (RMS) voltage at the point of common coupling (PCC), were used to control the charging and discharge processes. For both asymmetrical and symmetrical sag scenarios with various depths of sag, the efficiency of the suggested BES-based DVR was demonstrated. The suggested solution may also be highly beneficial for MG systems that supply electricity to delicate loads [33]-[35]. In [3], it was aimed to design and implement an effective PI controller for a DVR to address PQ issues. The optimal tuning of the PI controller was achieved using the artificial rabbit's optimization. The findings showed that the suggested system's parameters' waveforms (voltage, current, and power) were enhanced, and the system's performance was enhanced by keeping it running continuously during fault periods. To regulate wind power fluctuations and make up for disturbed grid voltages, another approach was proposed. The VSC compensates for fluctuations in grid voltage via the performance of the voltage injection and transformer, and the bidirectional converter controls power flow in both directions. Results for the wind energy conversion system's DVR-based ESS were verified using MATLAB/Simulink. The findings showed that the suggested strategy can adjust for disturbed grid voltages and regulate fluctuations of wind power [36], [37]. The effect of the voltage sag's phase jump characteristic regarding the load side following voltage sag recovers is mostly disregarded in current research, and existing DVR energy self-recovery techniques still have flaws. In order to reduce the total voltage compensation time, and rectify the phase jump, this study is presented, especially in wind and photovoltaic systems.

In this regard, the two situations used in this work; the main grid and demand, and the grid with wind and load, suggest a fresh approach for exploiting the DVR. This method assumes that the voltage of the load is near to or precisely the same as the nominal value. When considering different voltage imbalances, unbalanced and balanced sag/swell, notching, and other voltage disturbances, various fault states, and power system harmonic distortion. For controlling this compensator, the dynamic control technique proposes using an error-driven PI controller. Additionally, a proposed evaluation of performance using the honey badger algorithm (HBA) strategy regarding fault circumstances to obtain the suggested control method's global minimal error and fast-dynamic response. Simulations in the time domain using the Simulink/MATLAB platform have evaluated this DVR with the suggested controller.

The remainder of this paper is written as follows: Section 2 presents and discusses the system that is being studied in addition to models of their components. The proposed compensator and its working concept are described in detail in Section 3. Additionally, Section 3 presents and discusses the DVR modeling process as well as the process of design of the proposed PI controller. Section 4 discusses the formularization of the fitness function, the optimization problem, and the specific steps involved in the HBA. In Section 5, a performance evaluation of the proposed approach using offline time-domain simulations is presented. In Section 6 conclusions and suggested work extensions are presented. Table 1 shows the obtained results for the literature review and its evaluation, which summarizes that these studies do not provide a thorough evaluation of the system's performance, which includes variables such as PQ improvement, and reaction to various fault scenarios.

2. System Investigation

Fig. 1 illustrates a distribution system sample study including an 11 kV/ 0.4 kV, 1000 kVA, 50 Hz AC utility connected with a wind MG using a permanent magnet synchronous generator (PMSG). There are two busbars linked to the transformer's secondary windings. BUS 1 is connected through

a DVR circuit. Bus 2 is connected through a DVR circuit and non-linear load. The detailed specifications of the system components are shown in Table 2.

Table 1. The main results obtained from these studies

Reference	Main points	Evaluation
[23]	• The investigation of a DVR based on the MC with two three-phase inputs revealed its efficacy in correcting common PQ faults. • The suggested topology has several advantages, including compactness and an extended correction range. • The DVR's capacity to transport energy from an AF to the PF in a CPP enables the replacement of standard STS and DVR devices. • The DVR has better behavior and is an appealing tool for handling a wide range of disturbances influencing PQ energy, such as deep sags and voltage interruptions.	• The suggested DVR based on the MC with two three-phase inputs has several advantages, including compactness, increased compensation range, energy transfer capabilities, and enhanced general behavior, making it a potential solution for effective PQ disturbance compensation.
[26]	• The dynamic reaction of the DVR in three scenarios demonstrates that the DVR can correct voltage-related disruptions while the DC-link voltage is kept at its reference level. • In all circumstances, interruptions in supply voltage do not affect maintaining load voltage at the correct level.	• The evaluation shows that the load voltage remains steady at the correct level despite fluctuations in the supply voltage.
[28]	• The study concludes that utilizing a DVR series compensator controlled by a PI controller with the GTA optimization algorithm is an efficient approach for enhancing PQ issues related to RESs	• The study does not go into detail about the proposed control strategy's possible costs or actual implementation issues. The cost-effectiveness, feasibility, and compatibility of the DVR and control system with existing infrastructure and regulatory requirements should all be carefully considered.
[30]	• The dynamic energy management enabled by the RETO algorithm results in significant energy savings throughout the power distribution network. It also highlights an overall system efficiency improvement of 92.63%.	• It focuses on the RETO algorithm's optimization capabilities, energy efficiency, and harmonic distortion reduction.
[31]	• DVR served as an effective solution to address non-standard voltage, current, and frequency. • Simulations validated the proposed strategy's ability to mitigate voltage distortions caused by harmonics. • The study demonstrated the potential of DVR in improving power quality and protecting sensitive equipment.	• The study demonstrated the potential of DVR in improving power quality and protecting sensitive equipment but did not focus on the cost-effectiveness, or feasibility.
[32]	• The results show the successful operation of the hybrid energy storage (HES) based DVR for various voltage sag depth scenarios, including symmetrical and asymmetrical voltage imbalances.	• DVR systems based on HES might be costly to implement. Particularly for small-scale applications, the cost of the power electronics, control systems, and SMES may be a major barrier to practical deployment.
[33]	• The compensation demonstration of the proposed DVR system is carried out using power system computer-aided design (PSCAD/EMTDC) software. Simulation results validate the effectiveness of the system in mitigating symmetrical and asymmetrical voltage sag scenarios.	• The research work focuses only on voltage fluctuation enhancement for a sensitive load connected to a grid-integrated PV system. It does not address other PQ issues or consider scenarios beyond voltage sags.
[3]	• PQ problems caused by PV systems connecting to the power grid (PG) are successfully mitigated by the study effort. The suggested system, which consists of a DVR with a rotating dqRF controller and grid-tied PV, efficiently handles harmonics and faults to improve PQ and lessen their influence on customers.	• The scope does not encompass a broader range of PQ issues or consider the integration of other renewable energy sources.
[36]	• The DVR system successfully compensates for the disturbed voltages in the grid using the bidirectional converter and ESS.	• The description does not provide a thorough evaluation of the system's performance, which includes variables such as voltage stability, PQ improvement, and reaction to various fault scenarios.

It shows that non- linear load is 4.42 kW and 100 kVAR. The parameters of DVR are 500 Vdc, 1 Ω, 6 pulses for the VSC, and 10 mH and 20 µF for filter series inductance and capacitance, respectively.

Table 2. Detailed system component specifications

AC grid (utility)	50 Hz, 11 kV	
Transformer (T1)	1000 kVA, 11/0.4 kV	
Non-Linear Load	4.42 kW, 100 kVAR	
MG parameters	100 kVA, 0.4 kV	
DVR Parameters	DC Voltage	500 V
	R	.1 Ω
	f	50 Hz
	Voltage source inverter	6 pulses, 3 arms
	Filter series inductance	10 mH
	Filter series resistance	1 Ω
	Filter shunt resistance	1 Ω
	Filter shunt capacitance	20 µF
	Injection Transformer	1.5 kVA, .4 kV, a=1:1

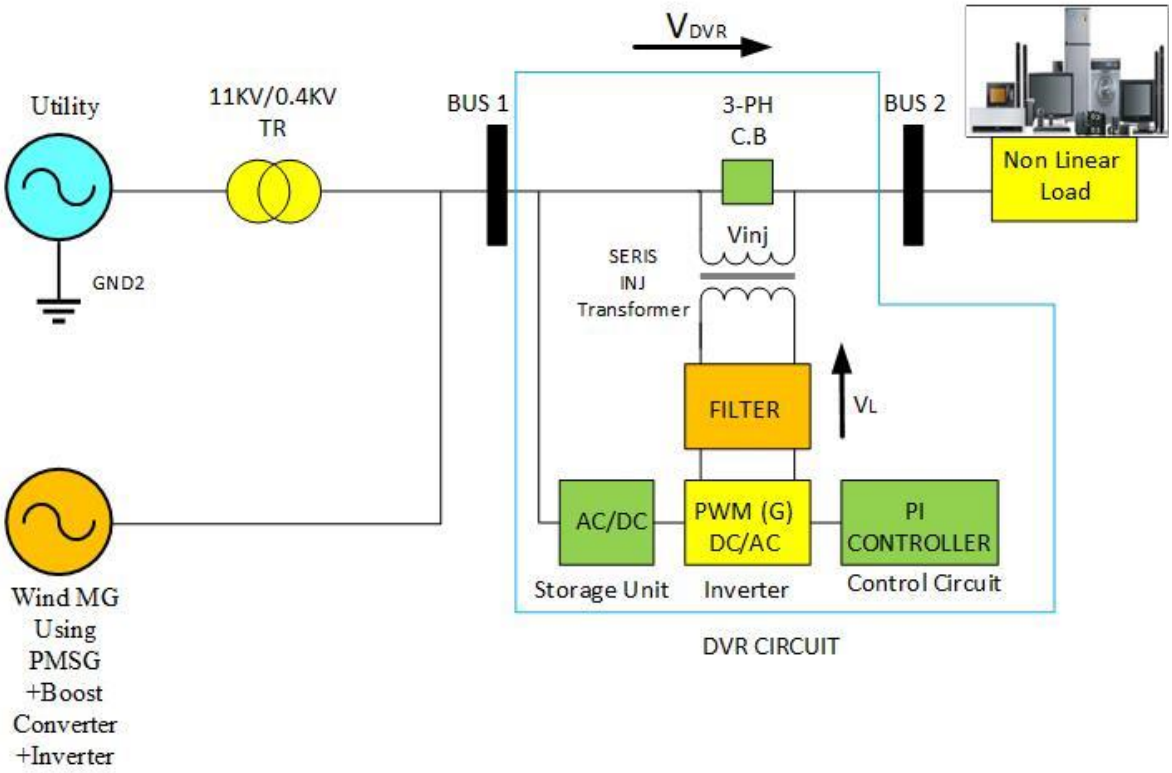

Fig. 1. Studied system

2.1. Wind Turbine (WT) Modeling

The extracted power from WTs can change based on:

$$P_m = P_W \times C_P \times C_f \times N_G \times N_B \quad (1)$$

$$P_W = 0.5 \times \pi \times \rho \times {V_W}^3 \times R^2 \quad (2)$$

where, P_m, and P_W is the mechanical and the WT power, respectively, ρ is the density of the air in kg/m3, V_W is the wind speed, and C_P is power coefficient, C_f is the capacity Factor, N_G is the generator's efficiency, and N_B is the gearbox efficiency. Fig. 2 & Fig. 3 show the rotation direction and power characteristics of the WT, respectively [38]-[43].

The system modeling in the MATLAB/Simulink platform in terms of improving unbalanced and balanced voltage swell and sag, as well as varied fault cases and transients' circumstances of the power system depicted in Fig. 4.

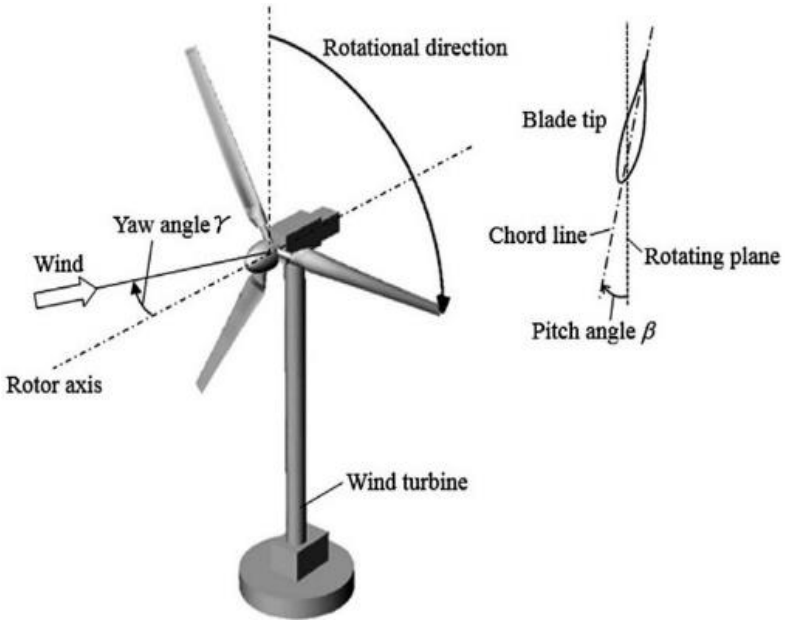

Fig. 2. The WT's direction of rotation

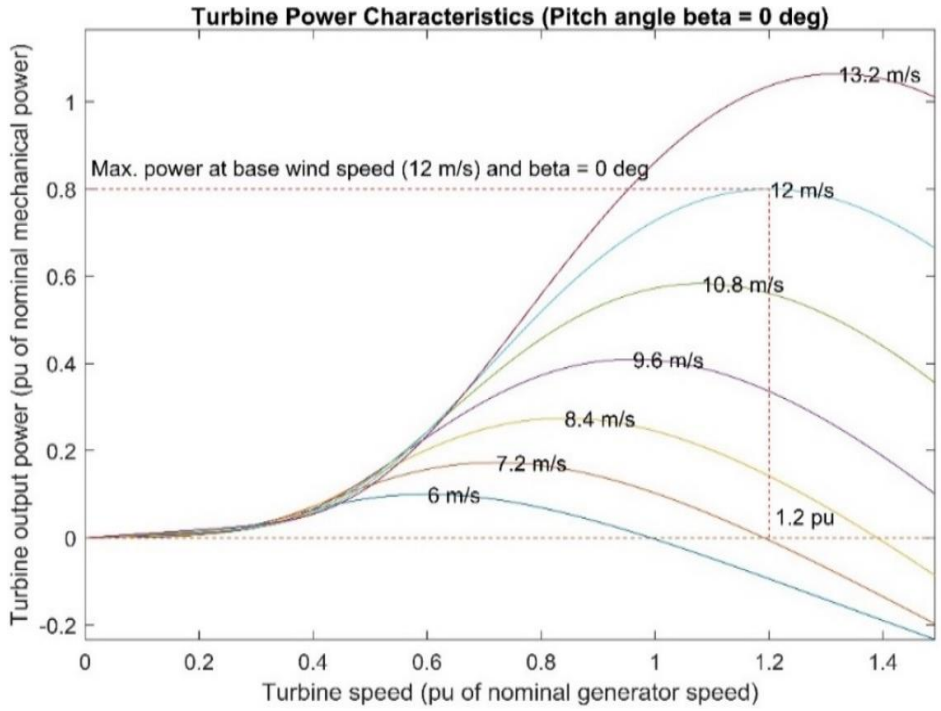

Fig. 3. WT power characteristics

2.2. Boost Converter (BC)

Fig. 5 shows the analogous circuit for the BC. It raises the Vout voltage from a lower input voltage. To do this, the necessary parts inductor, diode, and capacitor are placed in a different order. In comparison to transformer-based alternatives, this circuit's ability to greatly increase the input voltage. It also enables a more compact form factor. BCs continue to operate with high efficiency as well, especially at low voltage differentials. A further degree of system protection is added by the

inductor's intrinsic ability to limit inrush current [44]-[46].

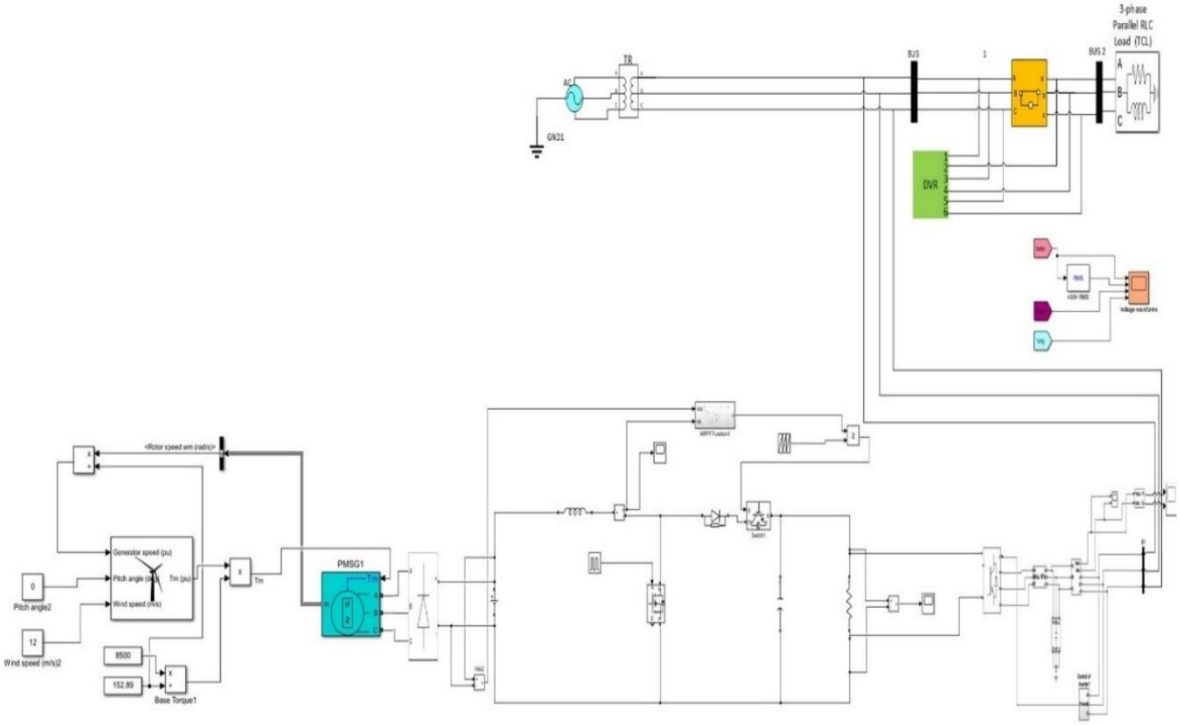

Fig. 4. Illustration of **s**imulation model in MATLAB

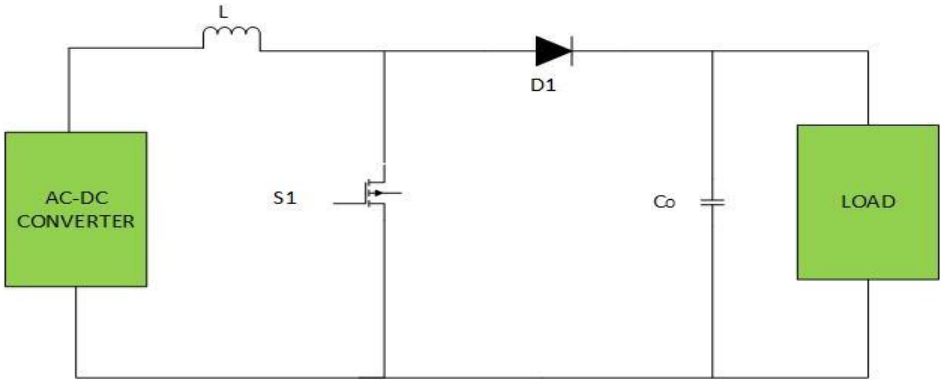

Fig. 5. Boost converter equivalent circuit

Table 3 illustrates the specification of the MG system components; the selected WT is of nominal mechanical output (8.5 kW) and fundamental wind speed (12 m/s). PMSG is 0.425 **Ω**, 0.000395 H, and 0.433 for stator resistance (R_s), armature inductance, and flux linkage, respectively. Inductor (L_B), capacitance (C_B), and resistance (R) for the BC are 12 V, 0.0000768 H, and 0.0004 F, respectively.

3. DVR Compensation

The proposed structure of DVR is placed amid the load buses (V_L and Vg). It functions as a PQ circumstance in parallel to increase voltage, reduce harmonic distortion, and compensate for reactive power. The three single-phase boosting transformers' AC sides are linked to a series capacitor, which is used to build the suggested DVR. A bank of capacitors and a series of resistances are connected in series to regulate the flow of electricity. The simulation of DVR system is depicted in Fig. 6, Fig. 7 shows DVR voltage compensation techniques. The proposed DVR system consists of the following components:

Table 3. MG system component specifications in detail

WT	Mechanical output power nominal (W)	8.5 kW
	The electrical generator base power (VA)	$8.5x10^3$/0.9 VA
	Fundamental wind speed (m/s)	12 m/s
	The base rotational speed of the base generator speed)	1.2 pu
	Pitch angle	0
PMSG	R_s	0.425 Ω
	Armature inductance	0.000395 H
	Flux linkage	0.433
BC	*Vdc*	12 V
	L_B	0.0000768 H
	C_B	0.0004 F
Filter circuit	R	4 Ω
	Filter series inductance	10 mH
	Filter series resistance	2 Ω
	Filter shunt capacitance	0.00135 F

- Energy storage unit: This unit provides the necessary real power to the DVR during voltage compensation. It can be implemented using supercapacitors or batteries, which offer fast response times and can serve as storage elements.
- Universal bridge unit: This power electronic device, also known as a VSC, converts the DC voltage from the energy storage unit to AC voltage. It ensures that the voltage injected into the transformer has the correct phase, magnitude, and frequency.
- Boosting transformer unit: This device steps up the voltage from the universal bridge unit to match the voltage level of the distribution network, enabling voltage compensation.
- Harmonic filter: This device minimizes harmonic distortion in the waveform generated by the VSI using an RLC circuit.
- PI controller: This controller monitors the load voltage and adjusts the DVR's output to maintain voltage stability.
- Bypass switch: This switch protects the DVR circuit from excessive currents by isolating it from the distribution network.

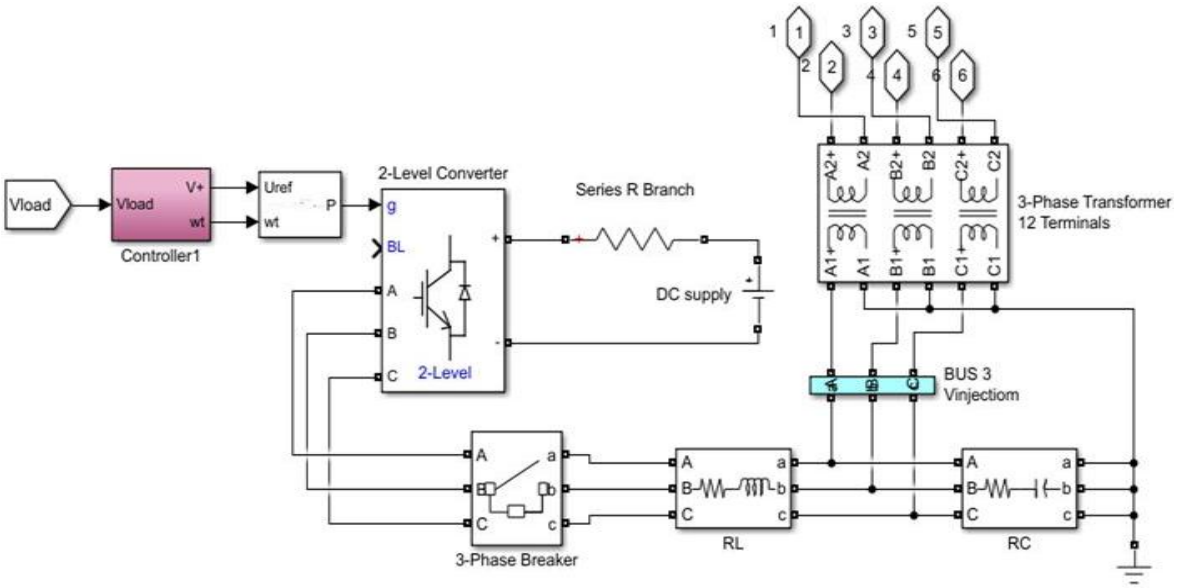

Fig. 6. The detailed simulation of the DVR system

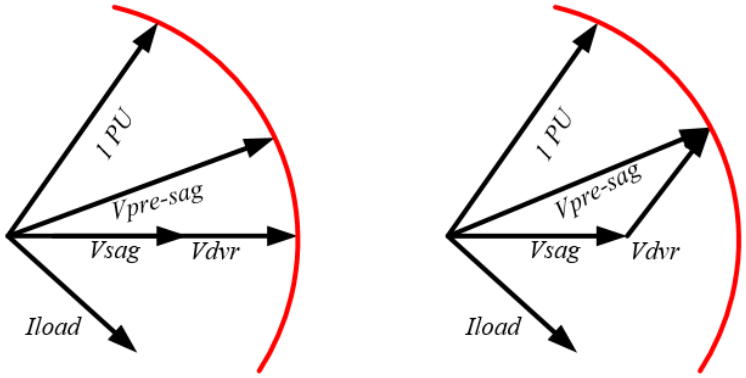

(a) (b)

Fig. 7. DVR voltage compensation techniques. (a) the technique of in-phase compensation, (b) a technique for compensating for pre-sag

3.1. The DVR Control Scheme Proposed

In general, the suggested DVR can be controlled in five steps, which are described below.

1. The system detects the voltage disturbances that take place.
2. As illustrated in Fig. 8, V_L is compared to a reference voltage.
3. The supply voltage and controller are in synch.
4. The controller scheme is presented.
5. The VSC, which absorbs growing voltage and compensates for dropping voltage, is driven by the gate pulses generated by the DVR voltages.

The type of voltage disturbance is crucial for recognizing depth, phase leap, and duration time (beginning and ending points). In this work, vectorized dq0 voltage components $V_{L,\,dq0}$ and $V_{ref,\,dq0}$ are created by applying Park transformation on the three-phase load voltage $V_{L,\,abc}$ and reference voltage $V_{ref,\,abc}$. The following formula is used to determine the three phases' reference voltages [47], [48]:

$$\begin{bmatrix} V_{A_{ref}} \\ V_{B_{ref}} \\ V_{C_{ref}} \end{bmatrix} = V_{L-max} \begin{bmatrix} \sin \omega t \\ \sin\left(\omega t - \frac{2\pi}{3}\right) \\ \sin\left(\omega t + \frac{2\pi}{3}\right) \end{bmatrix} \tag{3}$$

It is then converted from a three-phase abc-to-dq0 frame utilizing Park transformation, and this is described here:

$$\begin{bmatrix} V_d \\ V_q \\ V_0 \end{bmatrix} = \frac{2}{3} \begin{bmatrix} \cos(\omega t) & \cos\left(\omega t - \frac{2\pi}{3}\right) & \cos\left(\omega t + \frac{2\pi}{3}\right) \\ -\sin(\omega t) & -\sin\left(\omega t - \frac{2\pi}{3}\right) & -\sin\left(\omega t + \frac{2\pi}{3}\right) \\ \frac{1}{2} & \frac{1}{2} & \frac{1}{2} \end{bmatrix} \begin{bmatrix} V_a \\ V_b \\ V_c \end{bmatrix} \tag{4}$$

Once the load and reference voltages have been converted to the dq0 frame, they may be judged to determine the error signal, which is represented as a phase shift and voltage magnitude.

$$|e_{t,dq0}| = \sqrt{\left(V_{ref,d} - V_{L,d}\right)^2 + \left(V_{ref,q} - V_{L,q}\right)^2 + \left(V_{ref,0} - V_{L,0}\right)^2} \tag{5}$$

Any variation in the phase shift and magnitude of the voltage will result in a modification of the dq0 components. The suggested control swiftly recognizes variations in the state of the supply synchronization with the voltage of the supply is an important stage in achieving enough control over the DVR that is being shown. It maintains the controller's output signal in phase and frequency alignment through a reference input signal. As a result, the synchronization instrument used in this study is a phase-locked loop (PLL).

The described DVR control has low complexity because it is based on an error-driven PI control strategy. As seen in Fig. 9, the control function is to modify the error signal such that it is as small as possible on the distribution grid. Additionally, in the time domain, Vc which is defined as follows, is the contribution signal, which is provided here in the dq0 frame of the PWM of the DVR for the PI controller:

$$V_{c,dq0} = K_p\, e_{t,dq0} + K_i \int_0^1 e_{t,dq0}\, dt \tag{6}$$

Finally, the PI controller output returns to the three-phase abc frame to regulate the PWM that generates the gating pulses that desire the VSI, as shown below:

$$\begin{bmatrix} V_{c1,a} \\ V_{c1,b} \\ V_{c1,c} \end{bmatrix} = \begin{bmatrix} \sin(\omega t) & \cos(\omega t) & 1 \\ \sin(\omega t - \frac{2\pi}{3}) & \cos(\omega t - \frac{2\pi}{3}) & 1 \\ \sin(\omega t + \frac{2\pi}{3}) & \cos(\omega t + \frac{2\pi}{3}) & 1 \end{bmatrix} \begin{bmatrix} V_{c1,d} \\ V_{c1,q} \\ V_{c1,0} \end{bmatrix} \tag{7}$$

The control action of both the proportional and integral controllers is used in the proportional-integral controller. By combining these two different controllers, the inefficiencies of each are eliminated and a more effective controller is created. In this instance, the control signal exhibits proportionality with the error signal and its integral. The mathematical representation of the proportional plus integral controller is given as in equation (8) [49], [50]:

$$m(t) = k_d\, v(t) + k_{in} \int v(t) \tag{8}$$

For optimization of the PI controller, an energy storage system is used. The ESS reactive and active power performance When using ESS to increase power systems stability, PI controllers are crucial since the ESS must swiftly alter its active and reactive power, as shown in Fig. 9.

4. Application of Optimization Technique

4.1. Fitness Function

To fine-tune the recommended DVR-PI controllers' gains (K_p and K_i), the fitness function, as provided by Eq. (9), is defined as:

$$\min(E) = \min(ITAE) \tag{9}$$

where ITAE is the integral time absolute error and E is the total error of the proposed DVR's controller. The mathematical expression for the ITAE performance index is provided in Eq. (10):

$$ITAE = \int_0^\infty t\left|e_{t,dq0}\right| dt \tag{10}$$

where the error signal in the dq0 components between the load and reference voltages is represented by the symbol $e_{t,dq0}$The following limitations apply to the optimization problem:

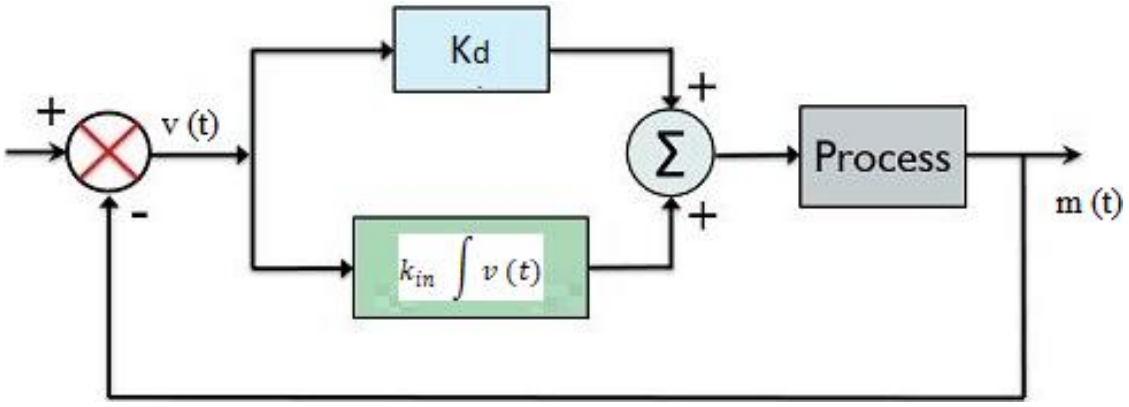

Fig. 8. The system block diagram with the PI controller

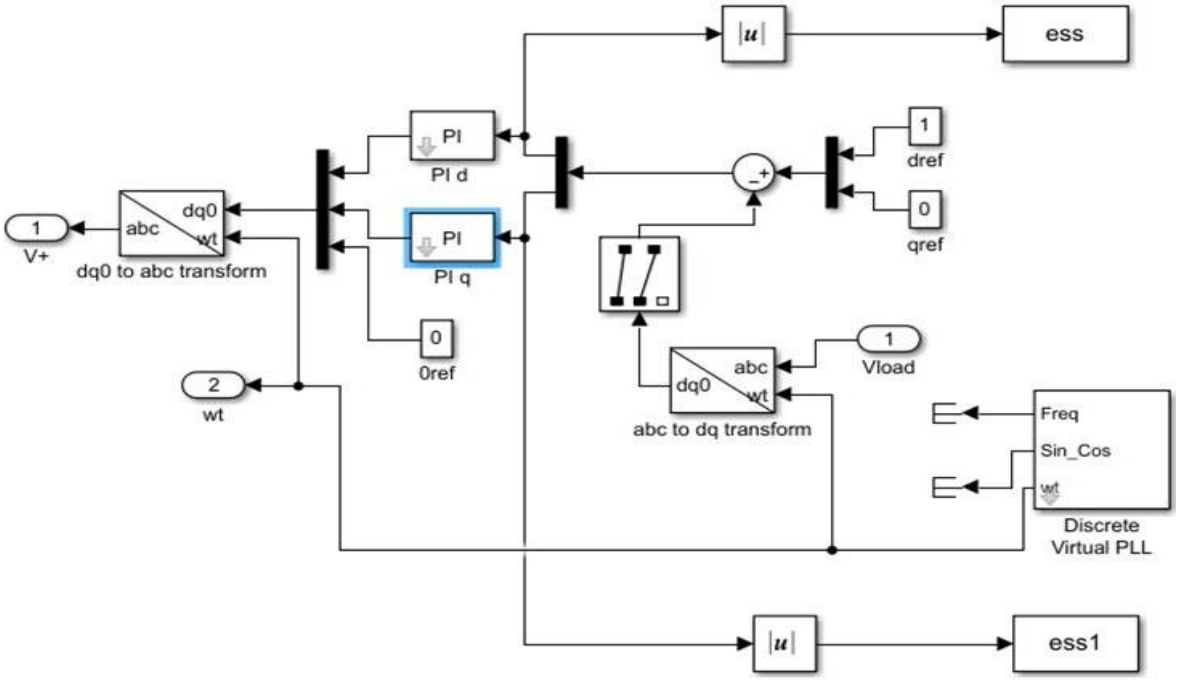

Fig. 9. The simulation of the optimized PI controller on MATLAB software

4.2. Constraints

- Eq. (11) restricts the level of voltage between the second feeder's maximum and minimum values, thus

$$0.95 \leq V_L \leq 1.05 \tag{11}$$

- The voltage's THD (THD_v), given by Eq. (12), ought to be less than its highest value ($THD_{v,max}$) reported in IEEE Standard 519, thus

$$THD_v = \frac{\sqrt{\sum_{h=2}^{n} V_h^2}}{V_1} \tag{12}$$

$$THD_v \leq THD_{v,max} \tag{13}$$

- The current THD (THD_i), given by Eq. (14), ought to be less than its highest value ($THD_{i,max}$) reported in IEEE Standard 519, thus

$$THD_i = \frac{\sqrt{\sum_{h=2}^{n} I_h^2}}{I_1} \quad (14)$$

$$THD_i \leq THD_{i,max} \quad (15)$$

4.3. Applied HBA

Using current meta-heuristic optimization techniques is one method of achieving the best answer to DVR control and improvement of the PQ. A fitness function is employed as a distance indication from the ideal solutions in the majority of these algorithms, which are based on natural events. The proposed reliability is restricted to DVR control and improvement of the PQ is solved through the use of a revolutionary HBA. It is a meta-heuristic search algorithm that finds motivation from how HBs use their clever foraging techniques to locate their meal. HBA formulates exploration as the dynamic-seeking behavior of an HB using methods of digging and honey finding. It would rather be by itself in self-dug tunnels, only coming together with other badgers for mating. When it is unable to flee, even much larger predators may attack it due to their bravery. It can also scale trees to get to beehives and bird nests so it can get food. The honeyguide bird, which can find the hives but cannot obtain honey, is followed by the honey badger, which finds its prey by excavating and using its ability to detect mice. HBs use two different ways to get to their food source: the first is termed "digging mode," and the second is called "honey mode." The HB uses its initiative to locate the hives in the first mode, but other birds assist it in the second technique. A relationship where both are reaping the benefits of teamwork is the result of the second mode phenomenon. Nonetheless, HBA's dynamic search modes stem from its capacity to uphold the equilibrium between exploration and exploitation during the search process. The representation of the HBA model in mathematics is as follows [51]-[53]:

The number of HBs is initially set according to individual size number (N) and their locations as follows in the first stage of the suggested HBA as equation (16):

$$HBP_i = lb_i(1 - r_1) + r_1 \times ub_i \quad (16)$$

where HBP is honey badger position, i is the number of iterations, ub, and lb are the upper and lower limits of each position. Then, the intensity (In) can be calculated as equation (17):

$$intensity_i = \frac{(r_2 \times (HBP_i - HBP_{i+1})^2)}{4\pi (HBP_{prey} - HBP_i)} \quad (17)$$

The density factor (α) is updated and adjusted to ensure a seamless transition from the exploration phase to the exploitation phase. It also controls the randomness of temporal variables. The way this factor decreases with additional rounds to lessen randomness over time is seen in (18):

$$Density\ factor = C\ (2)\ \times e^{\left(-\frac{t}{iter_{max}}\right)} \quad (18)$$

where $iter_{max}$ is a maximum iteration number, C is a constant equal to 2

A fag (F) that modifies the search direction is developed to improve escape from local to optima regions. However, agents now have multiple ways to fully go through the search space. Next, the positions of the agents are updated, and HBP_{new} is updated in accordance with the digging phase and the honeymoon phase. A honey badger's motions during the digging phase resemble the cardioid shape, which can be mimicked as in (19):

$$HBP_{new} = HBP_{prey}(1 + F * \beta * I) + F * r_4 * Density\ Factor * \left(HBP_{prey} - HBP_i\right) * |[1 - \cos 2\pi r_6] * \cos 2\pi r_5| \quad (19)$$

This algorithm is chosen because it offers a strong and effective method for improving PQ in distribution networks via DVR management, guaranteeing a more dependable and steady power source for customers. Determining the best control plan for the DVR system to reduce voltage fluctuations and improve PQ is the optimization problem. The goal is to minimize the voltage at the load buses' divergence from the intended reference voltage while meeting several requirements, including voltage limitations, DVR capacity, and system stability. The HBA optimizes the following parameters: the voltage injection's gain and phase angle and controls the DVR system's dynamic behavior. The best values for these parameters were determined using the optimization technique to reduce voltage deviations and enhance PQ. Optimizing the DVR device control approach is the main objective of the proposed solution, which aims to improve PQ in distribution networks. A power electronic device called a DVR is used in distribution networks to reduce voltage disturbances like swells and sags. To control and stabilize the voltage at the load buses, it injects voltage in series with the distribution line. The suggested algorithm seeks to maximize the DVR's compensation plan and control parameters to improve PQ and voltage restoration efficiency. The program looks for the best values for the control parameters and compensation technique by applying the HBOA and taking stability, system restrictions, and voltage variation into account. Fig. 9 shows the optimization procedures of the suggested method for improving PQ and controlling DVR robustly.

4.4. Execution of the HBA Technique

The HBA is utilized to fine-tune the controller gains for DVR control to ensure improved PQ performance in terms of voltage profile concerns like unbalanced and balanced swell/sag, diverse fault circumstances, and a decrease of harmonic distortion in the power system. As a result, the effect and value of the self-tuning PI control strategy in the act of the DVR the PI controller compares the dq0 components of VL with the V_{ref}, allowing the error signal to enter and the controller to compute the PI gains of this error signal. The DVR presence region is maximized and dynamic reaction is enhanced by the optimized controller. The chosen gains reduce the error signal to provide settled and effective reflexes to various disturbances. Additionally, the controller's outputs are converted into a V_{abc} frame and sent to a PWM generator. Therefore, by minimizing the error, the fitness function is selected to improve comprehensive performance. For this reason, comprehensive processes for determining the optimal solution.

After transferring from DC to AC via VSC, the boosting transformer will get the necessary phase angle and voltage injection from the storage element., ensuring improved PQ performance in terms of bus voltage improvement and stability, energy-efficient use, and harmonic distortion lessening in the system under consideration. The disturbance is what generates the error signal during fault conditions. Once the optimization loops were finished and the ideal resolution was obtained, the VSC turned on. During the healthy condition, the VSC will be off and the error signal will be nearly zero. Consequently, no voltage be injected by the storage element through the VSC to the boosting transformer. When searching for PI controller gains and calculating the global minimum error, the HBA-PI controllers' performance is verified using the following HBA parameters. Fig. 10 depicts the suggested application of the HBA for identifying controller parameters and obtaining global minimal error. Eight modes of operation are investigated for the simulation model: three different types of fault circumstances, unbalanced and balanced swell, and unbalanced and balanced sag. Table 4 contains detailed parameters for the optimized PI controller gains.

5. Results and Discussions

Two parameters, differing operating circumstances, and harmonic analysis, are provided to test the control methods. The load-side results are presented, and both the simulations with and without the suggested DVR are included. Additionally, a comparison is made between the ideal DVR performance of the used technique and the best solution for the optimized PI controllers' gains. Eight fault instances are simulated with the help of the MATLAB Simulink platform. The cases that are being studied can be summarized as follows:

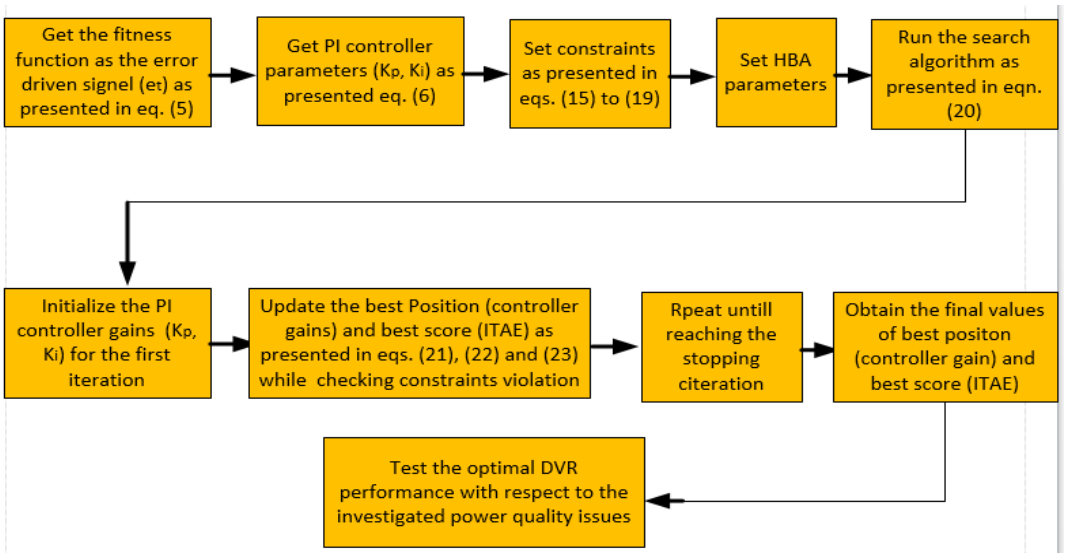

(a)

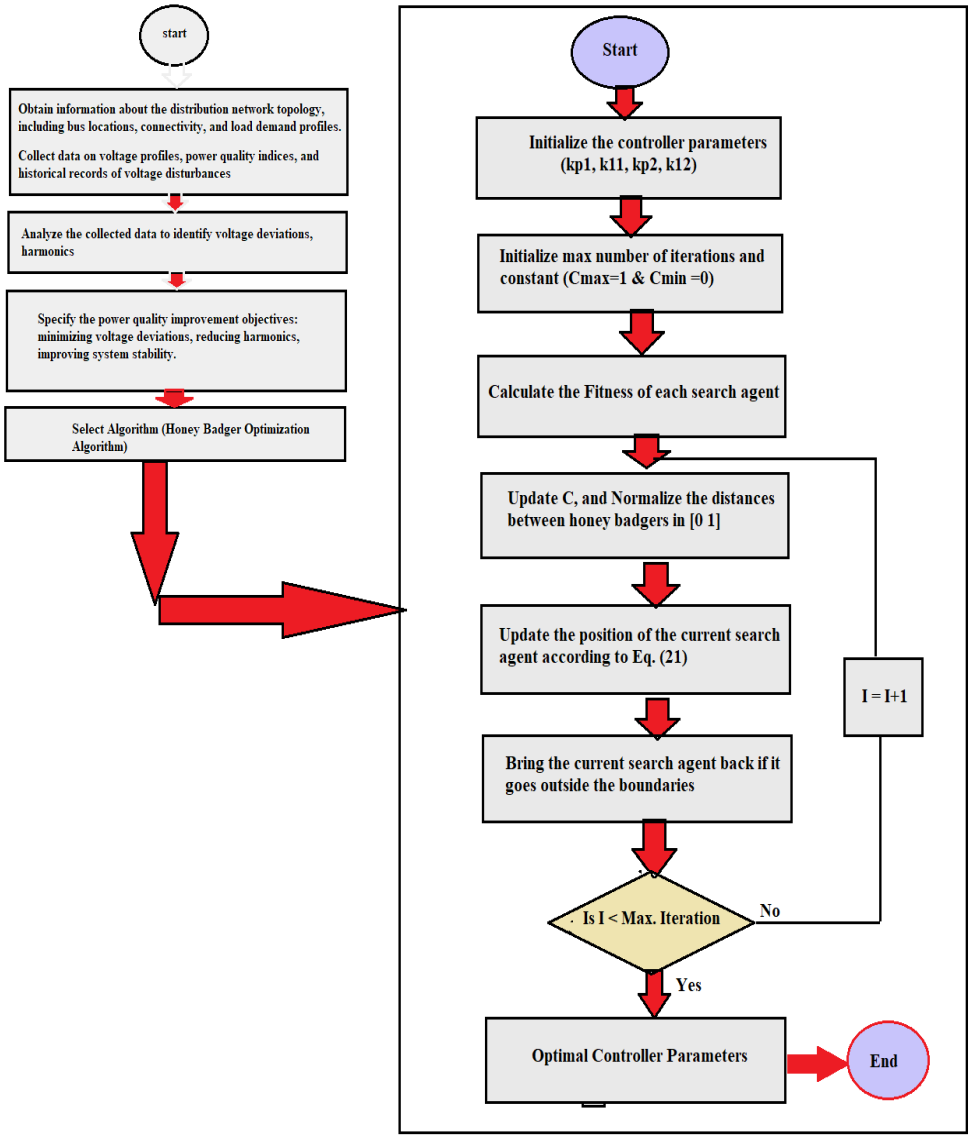

(b)

Fig. 10. Execution of the HBA: (a) the suggested application of the HBA (b) flowchart of the HBA

Table 4. HBA technique for determining the PI's optimal controller parameters

Conditions of operation	PI controller				Computation time (s)	Objective fn. (E)
	K_{p1}	K_{i1}	K_{P2}	K_{i2}		
Case 1: Balanced voltage sag	4.0460	2.2558	3.1559	0.6713	106.09	1.0476
Case 2: Unbalanced voltage sag	2.1144	2.3364	1.2740	0.5276	118.069	1.0447
Case 3: Balanced voltage swell	3.2381	1.7467	2.0229	1.0431	129.91	1.0745
Case 4: Unbalanced voltage swell	4.0736	1.9672	2.1937	2.2538	133.824	1.0475
Case 5: Three-phase short circuit	3.9013	1.6410	3.2216	0.9333	106.312	1.0476
Case 6: Double line - ground fault	1.7583	0.4865	0.5333	2.5591	116.062	1.0475
Case 7: Single line - ground fault	0.4276	0.1132	0.1527	0.1789	125.01	1.0476
Case 8: Analysis of Harmonic Distortions	4.1086	1.5433	4.2536	2.2159	124.972	1.0476

5.1. Case 1: Balanced Voltage Sag in Three Phases

The sag mode (SAM) arises in a three-phase balanced sag when certain heavy loads are turned off during each of the three phases. Consequently, it was supposed that the mode of sag would be utilized in this test. between time=0.20 and time=0.30 seconds. The voltage profile for each of the three phases during this event at the voltage bus for loads is depicted in the simulation results. The load voltage (V_L) after and before the DVR adjustment is shown in Fig. 11.

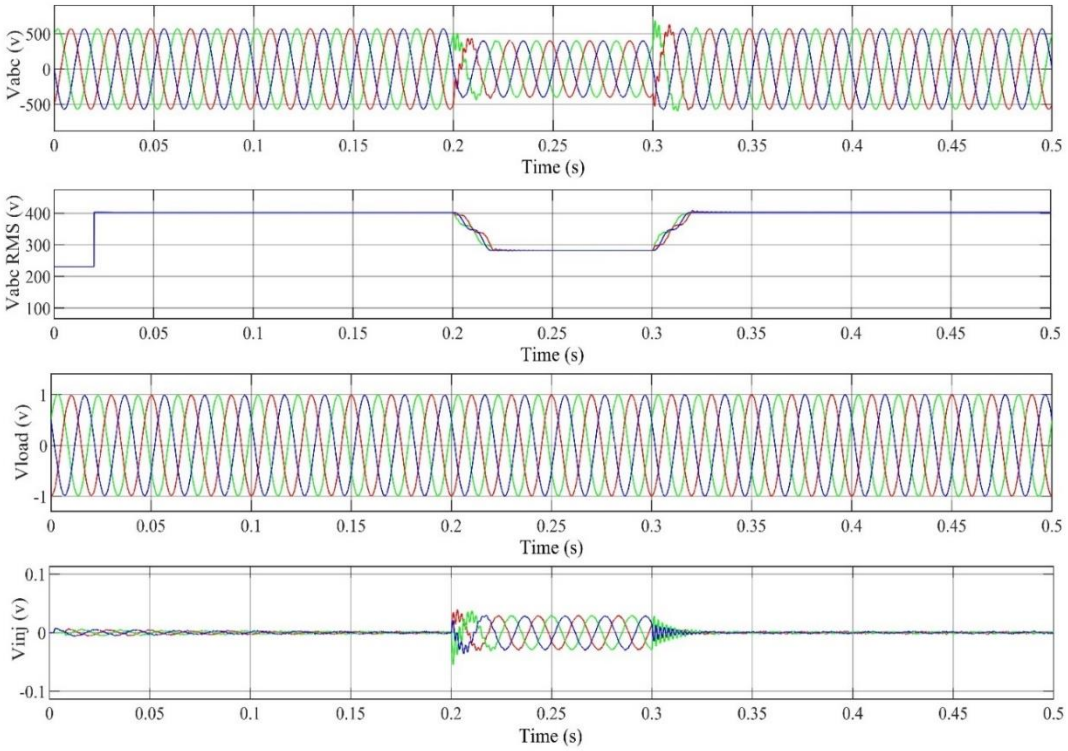

Fig. 11. Results for balanced sag: (a) V_L of the uncompensated load, (b) RMS-V_L of the uncompensated load (c) V_L of the compensated load, and (d) voltage injection

5.2. Case 2: Unbalanced (Single-Phase) Voltage Sag

Under the imbalanced SAM, phase A experiences an overload lasting 0.2 to 0.3 seconds. It should be emphasized, that the DVR quickly recognizes this sag state throughout several phases and inserts the essential phase angle and amplitude of voltage to maintain V_L balanced. Fig. 12 illustrates the V_L profile before and post decompensation, in addition to the needful injection voltage.

5.3. Case 3: Balanced Voltage Swells in Three Phases

A swell mode (SWM) known as a three-phase balanced swell occurs when various heavy loads shut down in three phases. As a result, it was supposed that the mode of swell would be utilized in

this test from time=0.20 s to time=0.30 s. The simulation results demonstrate the voltage profile at this load voltage bus during the three phases of this case. Fig. 13 illustrates the V_L profile before and post decompensation utilizing a DVR.

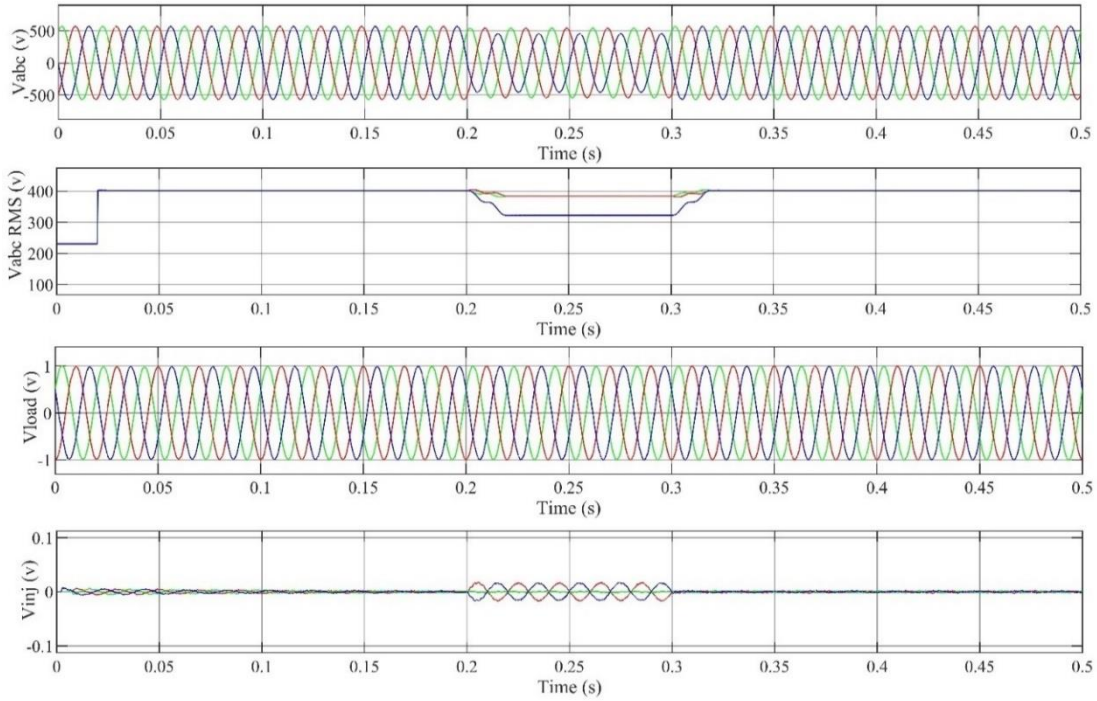

Fig. 12. Results for the unbalanced sag: (a) V_L of the uncompensated load, (b) RMS-V_L of the uncompensated load (c) V_L of the compensated load, and (d) voltage injection

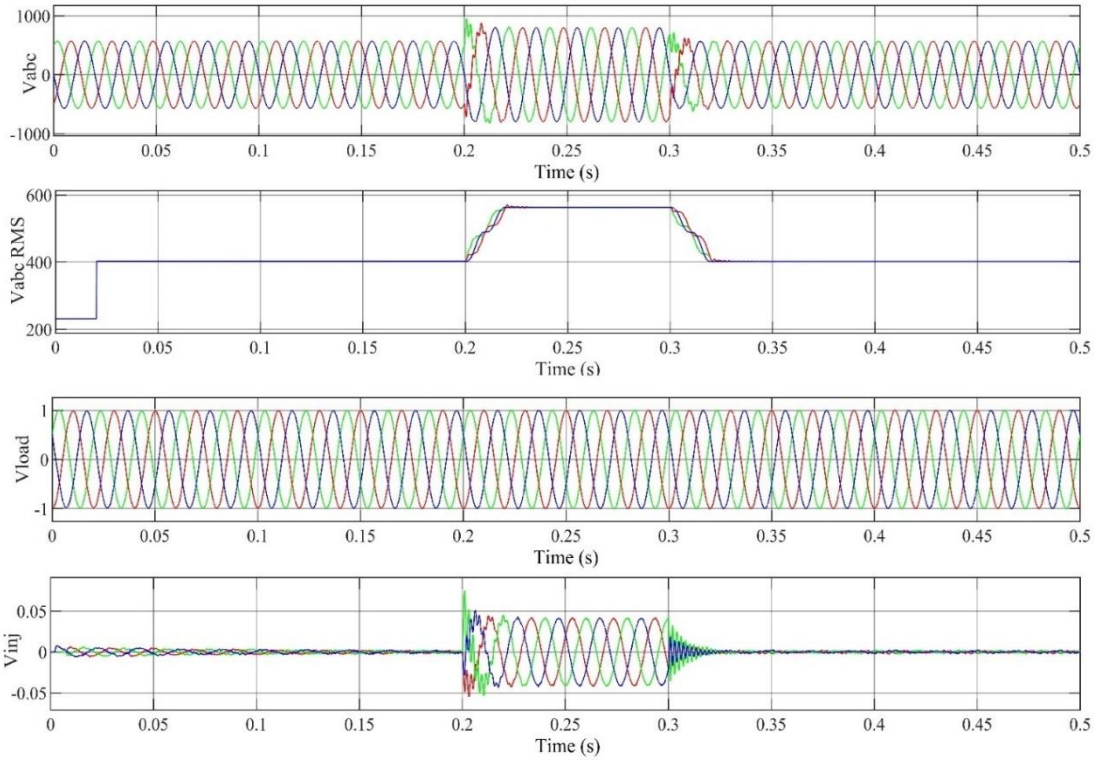

Fig. 13. Results for balanced swell: (a) V_L of the uncompensated load, (b) RMS-V_L of the uncompensated load (c) V_L of the compensated load, and (d) voltage injection

5.4. Case 4: Unbalanced (Single-Phase) Voltage Swell

Under unbalanced swell mode, an overload happens from 0.20 s to 0.30 s. It should be emphasized, that the DVR quickly recognizes this swell state throughout several phases and inserts the needed phase angle and amplitude of voltage to maintain V_L balanced. Fig. 9 illustrates the V_L profile prior to and post decompensation, in order to the needful injection voltage. When the DVR is displayed during this event, Fig. 14 shows how the DVR improves the V_L profile of the system under research by injecting the required voltage on each of the three phases.

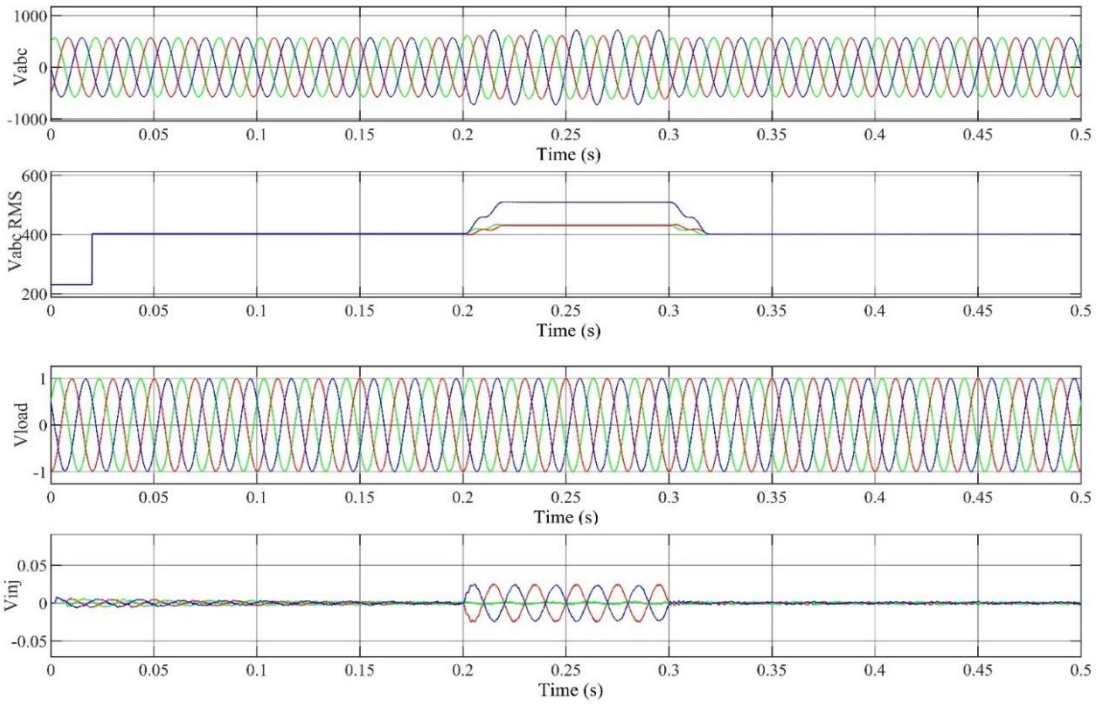

Fig. 14. Results for unbalanced swell: (a) V_L of the uncompensated load, (b) RMS-V_L of the uncompensated load (c) V_L of the compensated load, and (d) voltage injection

5.5. Case 5: Three-Phase Short Circuit (TL-G)

According to the phase short circuit, Fig. 15 represents the voltage profile at V_L before and after decompensation.

5.6. Case 6: Double Line to Ground Fault (DL-G)

At the first feeder, there is a double line-to-ground fault between t=0.2 and t=0.3 seconds. In this failure state, the DVR swiftly injects the appropriate voltage. Fig. 16 shows the voltage profiles at V_L before and after decompensation, as well as the injected voltage.

5.7. Case 7: Single Line to Ground Fault (SL-G)

There is a single line-to-ground fault between t=0.2 and t=0.3 seconds. During this occurrence, there is a balanced fault (three phases of equal voltage). The voltage profile at V_L after and before adjustment is shown in Fig. 17.

5.8. Case 8: Analysis of Harmonic Distortions

When gauging the degree of harmonic distortion of the voltage or current waveforms, THD is a crucial metric. Thus, using the recommended DVR, THD values at the source and load buses for voltage and current will be examined as illustrated in Fig. 18.

Fig. 19 shows the gauging THD of the voltages at the load bus (VL) under various operating conditions, both before and after compensation, to confirm the efficacy of the suggested DVR

scheme. As can be observed, results for various scenarios; swell mode (SWM) with DVR, SWM without DVR, and sag mode (SAM) with DVR are shown.

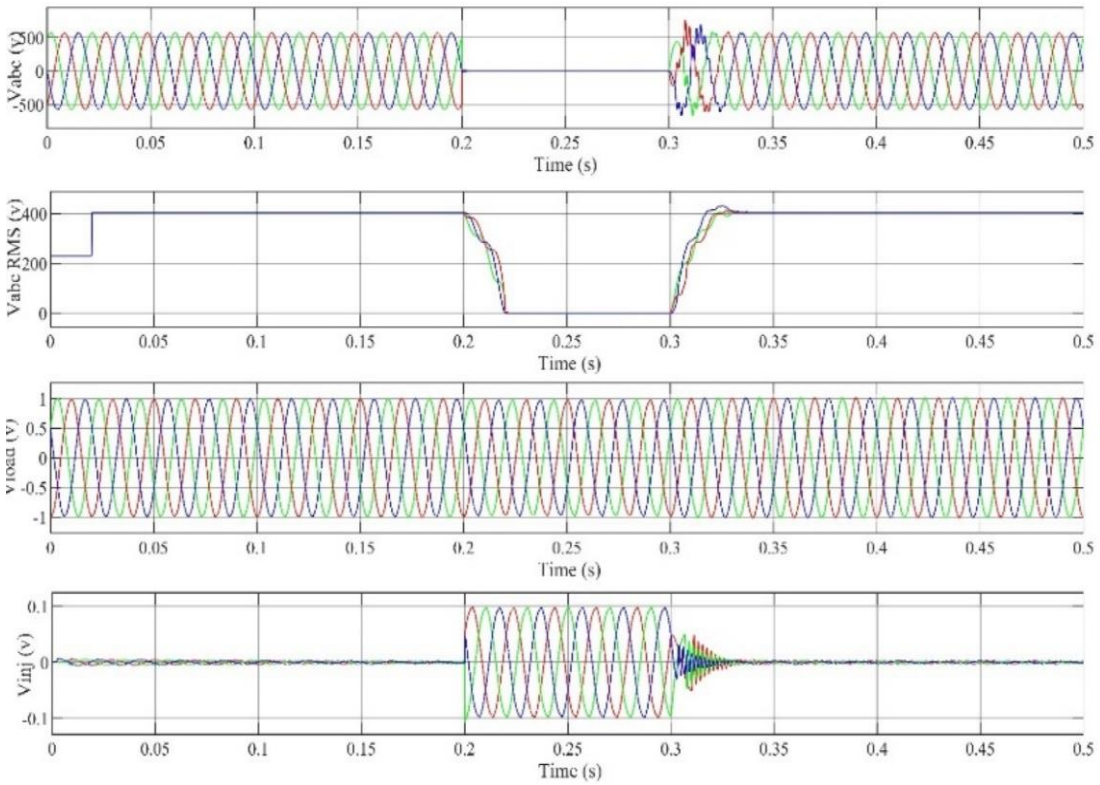

Fig. 15. Results for Three-phase short circuit: (a) V_L of the uncompensated load, (b) RMS-V_L of the uncompensated load (c) V_L of the compensated load, and (d) voltage injection

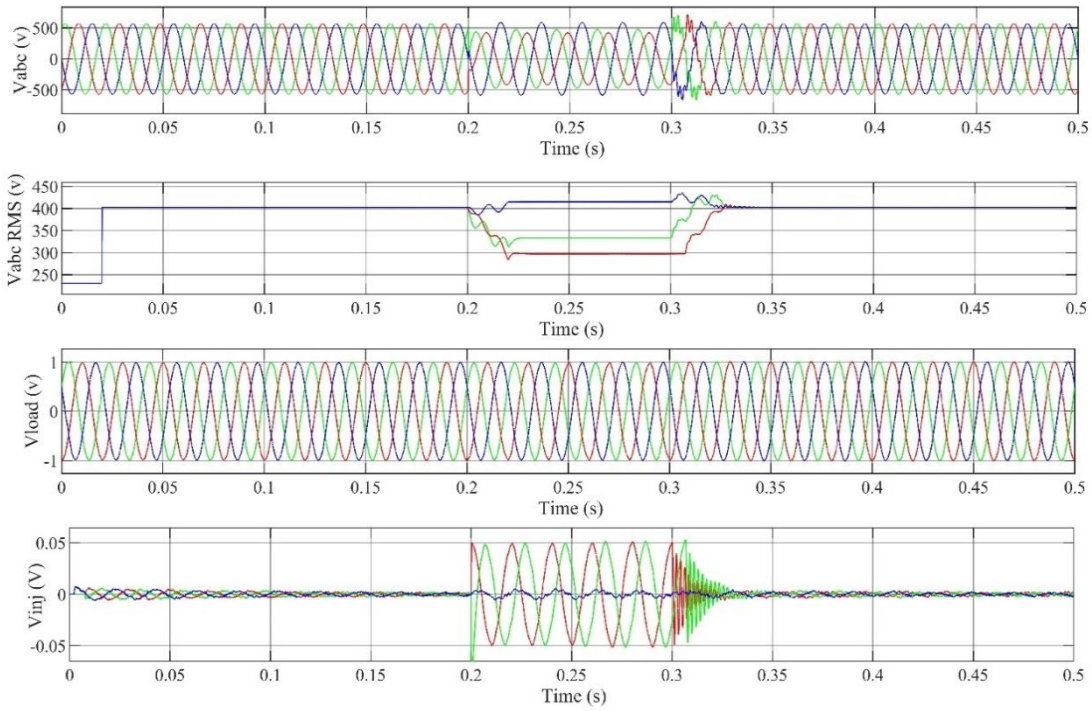

Fig. 16. Results for a double line to ground: (a) V_L of the uncompensated load, (b) RMS-V_L of the uncompensated load (c) V_L of the compensated load, and (d) voltage injection

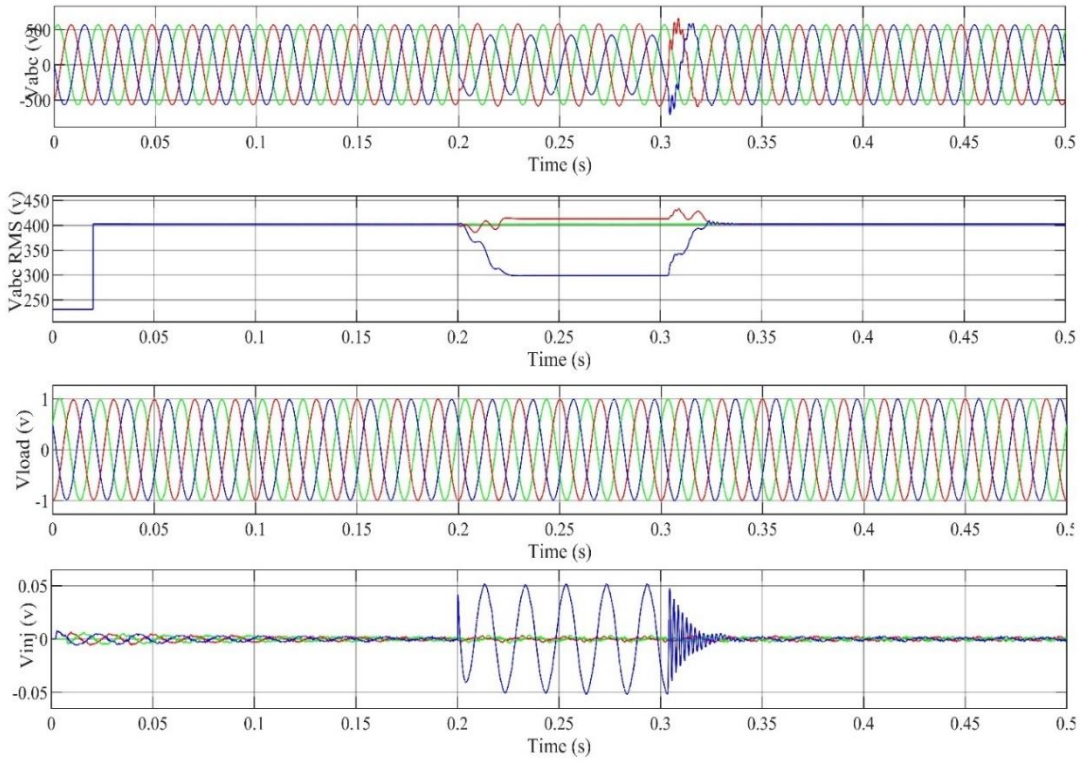

Fig. 17. Results for single line to ground fault: (a) V_L of the uncompensated load, (b) RMS-V_L of the uncompensated load (c) V_L of the compensated load, and (d) voltage injection

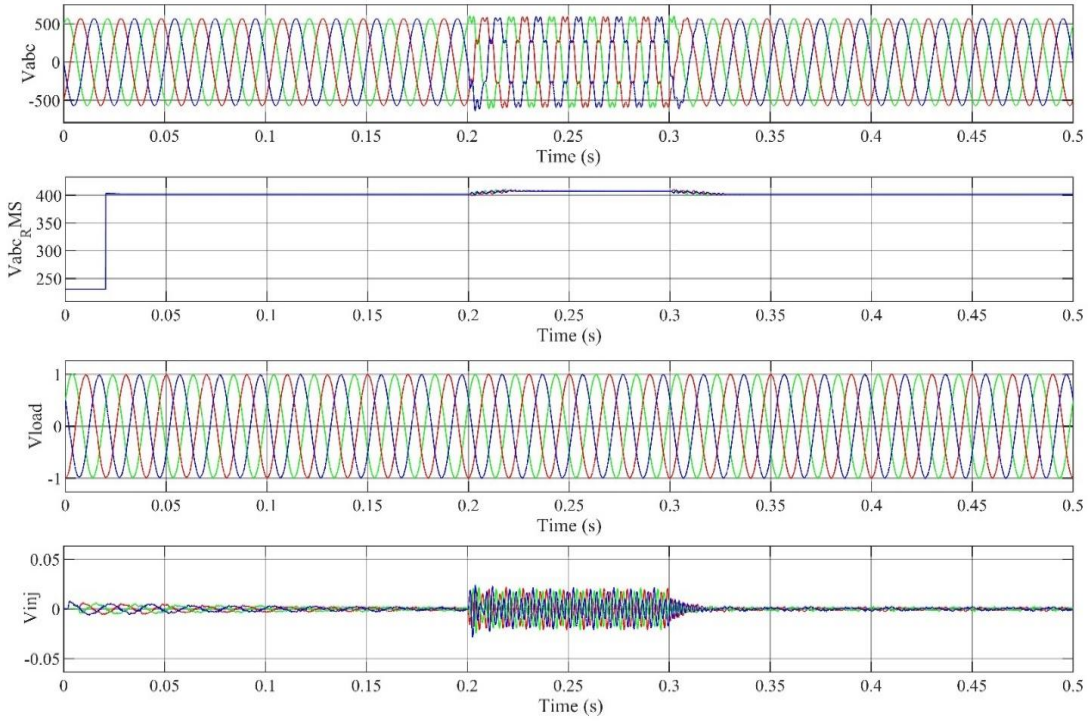

Fig. 18. Results for harmonic distortion mode: (a) V_L of the uncompensated load, (b) RMS-V_L of the uncompensated load (c) V_L of the compensated load, and (d) voltage injection

The distortion contained in the voltage waveform is measured by THDv, which is the subject of the investigation. THDv at VL in SAM with DVR: This is the THDv measurement at the VL during

a voltage sag in the system while the DVR is in operation. The amount of harmonic distortion in this case's voltage waveform is indicated by the THDv value. When there is a voltage drop in the system while the DVR is operating, the THDv measurement at the VL is shown in Fig. 19 (a). When there is a voltage drop in the system but the DVR is not in use, the THDv measurement at the VL is shown in Fig. 19 (b). Without the DVR's compensatory effect, the THDv number indicates the degree of harmonic distortion in the voltage waveform in this case. When the DVR is operating and there is a voltage swell in the system, the THDv measurement at the VL is shown in Fig. 19 (c). With the DVR correcting for the voltage, the THDv number shows the degree of harmonic distortion in the voltage waveform during this swell occurrence. When there is a voltage spike in the system but the DVR is not in use, the THDv measurement at the VL is shown in Fig. 19 (d). Without the DVR's compensatory effect, the THDv value indicates the degree of harmonic distortion in the voltage waveform during the swell event. The efficacy of the DVR in minimizing harmonic distortions during voltage sags and swells was assessed by comparing these THDv values under various conditions. Better voltage quality and less distortion are indicated by a lower THDv value.

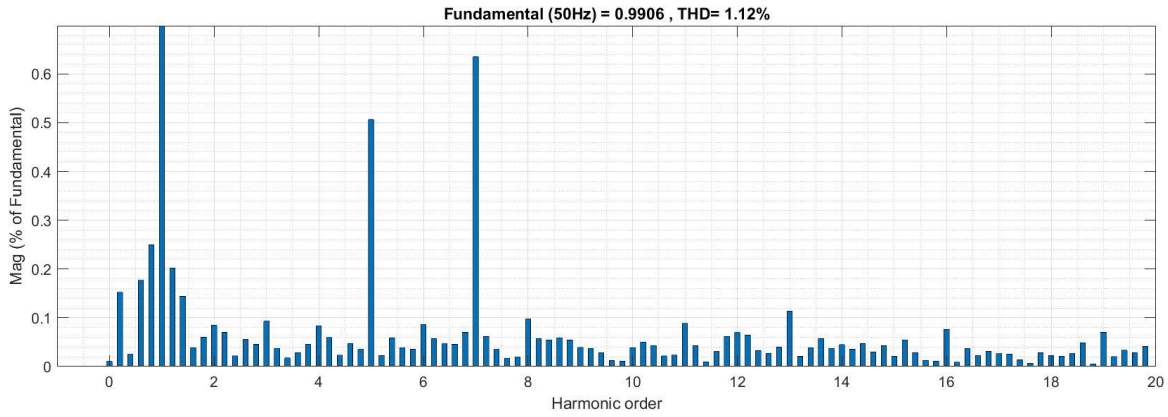

(a)

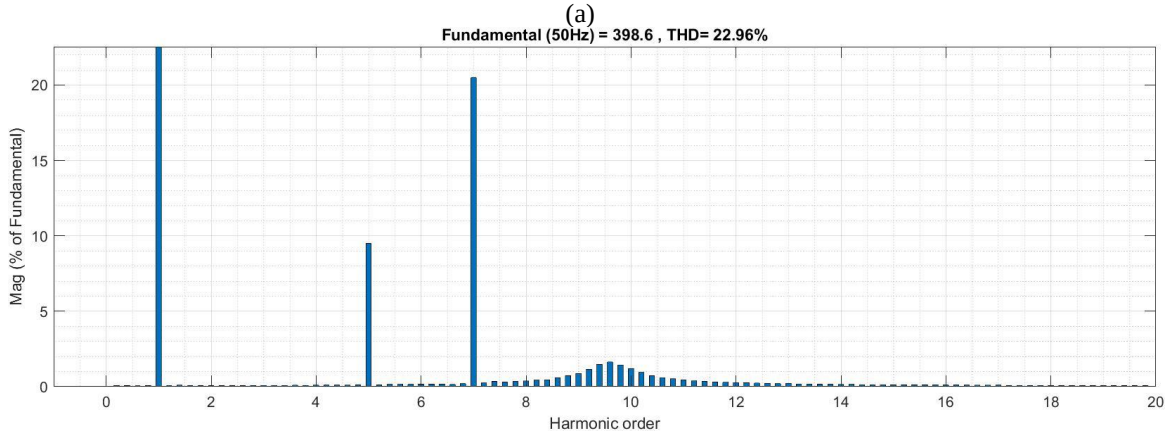

(b)

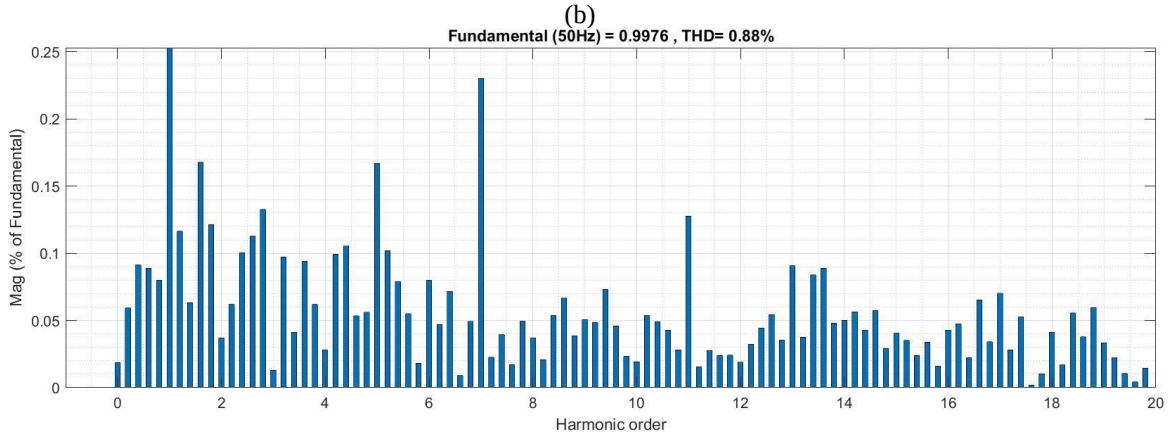

(c)

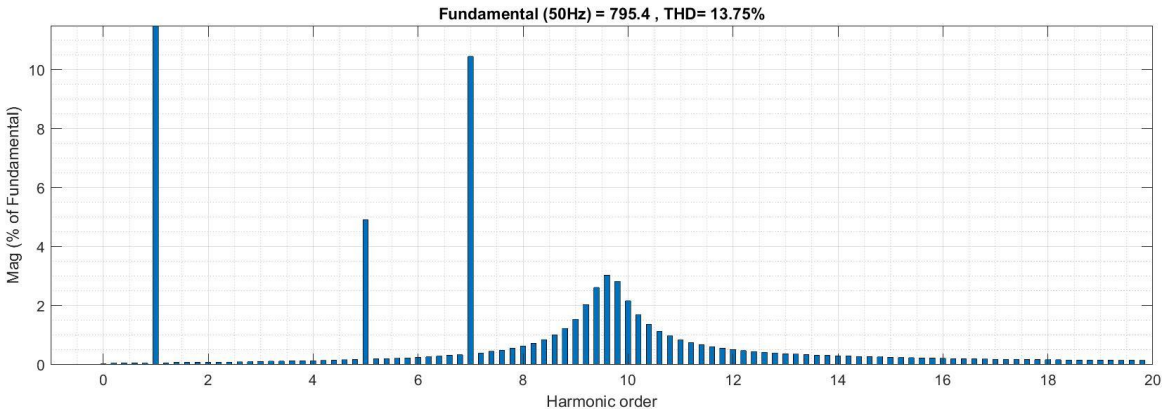

(d)

Fig. 19. Voltage investigation at the VL using FFT: (a) *THDv* in sag mode at VL with DVR, (b) THD_v at V_L without DVR in sag mode, (c) THD_v at V_L with DVR during swell mode, (d) THD_v at V_L without DVR during swell mode

Internal threats in this study include the improper selection of algorithm parameters, such as population size or mutation rate, which can result in poor solutions or premature convergence. Furthermore, the presence of local optima or the algorithm's sensitivity to beginning conditions may influence the robustness and trustworthiness of the results. External threats indicate the likelihood of considerable variations in distribution network topology, load characteristics, and operating conditions between areas or periods. As a result, the HBA's efficiency in enhancing PQ via DVR control may vary depending on network setup or interruptions. While the results reported for the HBA in improving PQ via DVR management are encouraging, it is important to recognize internal and external challenges to the results' trustworthiness.

6. Conclusions

Utilizing a DVR system as a series compensated scheme, the research offers a novel low-cost voltage management solution to address PQ disputes of hybrid industrial loads linked to a distribution network. This guarantees energy-efficient functioning and little effect on the grid schemes. To minimize the overall error-driven loop and ensure quick, dynamic reaction to the purpose of effective energy use, the voltage source inverter's switching signal is driven by the DVR scheme, which is managed by an optimal PI regulation controller. To validate the suggested method, a fractional order PI is shown and contrasted with a normal PI. Additionally, the MATLAB/Simulink platform's system modeling is used to enhance balanced and imbalanced voltage sag and swell, as well as various fault scenarios and transient conditions for the power system. It is discovered that this approach's performance can improve power quality.

In subsequent research, the same device will be expanded to include a multi-stage, recently refined metaheuristic-based controller and changeable structure-sliding mode—Bang Bang—for use in smart systems that integrate hybrid fuel cells, photovoltaic cells, and supercapacitors. Furthermore, new DVR inter-coupled- AC/DC compensation system topologies going to be created. The following are the anticipated trends:

1. An emphasis on creating sophisticated DVR system control schemes. This includes investigating intelligent control methods like artificial intelligence, machine learning, and sophisticated algorithms.
2. Future trends call for the integration of DVR systems with renewable energy systems as renewable energy sources become more and more prevalent in distribution networks.
3. Future developments in grid resilience will involve the incorporation of DVR systems into robust distribution networks and microgrids.

Author Contribution: All authors contributed equally to the main contributor to this paper. All authors read and approved the final paper.

Funding: This research received no external funding.

Conflicts of Interest: The authors declare that they have no conflicts of interest.

Data Availability: The data used to support the findings of this study are available at reasonable request from the corresponding author.

References

[1] O. J. Singh and D. P. Winston, "Enhanced Method of Mitigating Voltage Sags and Swells Using Optimized Fuzzy Controlled DVR," *Iranian Journal of Science and Technology, Transactions of Electrical Engineering*, vol. 47, pp. 147-158, 2023, https://doi.org/10.1007/s40998-022-00556-8.

[2] M. Awad *et al.*, "A review of water electrolysis for green hydrogen generation considering PV/wind/hybrid/hydropower/geothermal/tidal and wave/biogas energy systems, economic analysis, and its application," *Alexandria Engineering Journal*, vol. 87, pp. 213-239, 2024, https://doi.org/10.1016/j.aej.2023.12.032.

[3] N. F. Ibrahim, A. Alkuhayli, A. Beroual, U. Khaled, and M. M. Mahmoud, "Enhancing the Functionality of a Grid-Connected Photovoltaic System in a Distant Egyptian Region Using an Optimized Dynamic Voltage Restorer: Application of Artificial Rabbits Optimization," *Sensors*, vol. 23, no. 16, p. 7146, 2023, https://doi.org/10.3390/s23167146.

[4] R. Kassem *et al.*, "A Techno-Economic-Environmental Feasibility Study of Residential Solar Photovoltaic / Biomass Power Generation for Rural Electrification : A Real Case Study," *Sustainability*, vol. 16, no. 5, p. 2036, 2024, https://doi.org/10.3390/su16052036.

[5] M. M. Mahmoud *et al.*, "Voltage Quality Enhancement of Low-Voltage Smart Distribution System Using Robust and Optimized DVR Controllers : Application of the Harris Hawks Algorithm," *International Transactions on Electrical Energy Systems*, vol. 2022, no. 1, pp. 1-18, 2022, https://doi.org/10.1155/2022/4242996.

[6] M. M. Mahmoud *et al.*, "Application of Whale Optimization Algorithm Based FOPI Controllers for STATCOM and UPQC to Mitigate Harmonics and Voltage Instability in Modern Distribution Power Grids," *Axioms*, vol. 12, no. 5, p. 420, 2023, https://doi.org/10.3390/axioms12050420.

[7] M. M. Hussein, T. H. Mohamed, M. M. Mahmoud, M. Aljohania, M. I. Mosaad, and A. M. Hassan, "Regulation of multi-area power system load frequency in presence of V2G scheme," *PLoS One*, vol. 18, no. 9, p. e0291463, 2023, https://doi.org/10.1371/journal.pone.0291463.

[8] N. Kassarwani, J. Ohri, and A. Singh, "Comparative Performance Study of DVR Using Adaptive LMS Filtering-Based Algorithms," *Electric Power Components and Systems*, vol. 52, no. 7, pp. 1054-1081, 2024, https://doi.org/10.1080/15325008.2023.2238694.

[9] A. H. Soomro, A. S. Larik, A. A. Sahito, M. A. Mahar, and I. A. Sohu, "Simulation-based Analysis of a Dynamic Voltage Restorer under Different Voltage Sags with the Utilization of a PI Controller," *Engineering, Technology and Applied Science Research*, vol. 10, no. 4, pp. 5889-5895, 2020, https://doi.org/10.48084/etasr.3524.

[10] M. M. Mahmoud, M. M. Aly, H. S. Salama, and A. M. M. Abdel-Rahim, "Dynamic evaluation of optimization techniques–based proportional–integral controller for wind-driven permanent magnet synchronous generator," *Wind Engineering*, vol. 45, no. 3, pp. 696-709, 2021, https://doi.org/10.1177/0309524X20930421.

[11] L. Saribulut and A. Ameen, "Voltage Sag Detection and Compensation Signal Extraction for Power Quality Mitigation Devices," *Energies*, vol. 16, no. 16, p. 5999, 2023, https://doi.org/10.3390/en16165999.

[12] O. M. Kamel, A. A. Z. Diab, M. M. Mahmoud, A. S. Al-Sumaiti, and H. M. Sultan, "Performance Enhancement of an Islanded Microgrid with the Support of Electrical Vehicle and STATCOM Systems," *Energies*, vol. 16, no. 4, p. 1577, 2023, https://doi.org/10.3390/en16041577.

[13] S. A. Mohamed, N. Anwer, and M. M. Mahmoud, "Solving optimal power flow problem for IEEE-30 bus system using a developed particle swarm optimization method: towards fuel cost minimization," *International Journal of Modelling and Simulation*, pp. 1-14, 2023, https://doi.org/10.1080/02286203.2023.2201043.

[14] S. N. Setty, M. S. D. Shashikala, and K. T. Veeramanju, "Hybrid control mechanism-based DVR for mitigation of voltage sag and swell in solar PV-based IEEE 33 bus system," *International Journal of Power Electronics and Drive Systems*, vol. 14, no. 1, pp. 209-221, 2023, https://doi.org/10.11591/ijpeds.v14.i1.pp209-221.

[15] N. F. Ibrahim *et al.*, "Operation of Grid-Connected PV System With ANN-Based MPPT and an Optimized LCL Filter Using GRG Algorithm for Enhanced Power Quality," *IEEE Access*, vol. 11, pp. 106859-106876, 2023, https://doi.org/10.1109/ACCESS.2023.3317980.

[16] M. M. Mahmoud, M. M. Aly, H. S. Salama, and A.-M. M. Abdel-Rahim, "An internal parallel capacitor control strategy for DC-link voltage stabilization of PMSG-based wind turbine under various fault conditions," *Wind Engineering*, vol. 6, no. 3, pp. 983-992, 2022, https://doi.org/10.1177/0309524X211060684.

[17] H. Abdelfattah *et al.*, "Optimal controller design for reactor core power stabilization in a pressurized water reactor: Applications of gold rush algorithm," *PLoS One*, vol. 19, no. 1, p. e0296987, 2024, https://doi.org/10.1371/journal.pone.0296987.

[18] M. M. Mahmoud *et al.*, "Evaluation and Comparison of Different Methods for Improving Fault Ride-Through Capability in Grid-Tied Permanent Magnet Synchronous Wind Generators," *International Transactions on Electrical Energy Systems*, vol. 2023, no. 1, pp. 1-22, 2023, https://doi.org/10.1155/2023/7717070.

[19] Z. Li, X. Guo, Z. Wang, R. Yang, and G. Chen, "A fast switching strategy for DVR based on current control algorithm," *Energy Reports*, vol. 9, pp. 584-593, 2023, https://doi.org/10.1016/j.egyr.2022.12.111.

[20] A. Moghassemi and S. Padmanaban, "Dynamic voltage restorer (DVR): A comprehensive review of topologies, power converters, control methods, and modified configurations," *Energies*, vol. 13, no. 6, p. 4152, 2020, https://doi.org/10.3390/en13164152.

[21] T. Thongsan and T. Chatchanayuenyong, "A Simple and Fast Voltage Disturbance Detection and Voltage Reference Generation Approach for Dynamic Voltage Restorer (DVR) to Compensate Unbalanced Voltage Sag and Swell in Three-Phase System: Simulation and Experimental Testing," *ECTI Transactions on Electrical Engineering, Electronics, and Communications*, vol. 21, no. 1, pp. 1-15, 2023, https://doi.org/10.37936/ecti-eec.2023211.248611.

[22] N. Mbuli, "Dynamic Voltage Restorer as a Solution to Voltage Problems in Power Systems: Focus on Sags, Swells and Steady Fluctuations," *Energies*, vol. 16, no. 19, p. 6946, 2023, https://doi.org/10.3390/en16196946.

[23] S. C. Yáñez-Campos, G. Cerda-Villafaña, and J. M. Lozano-Garcia, "Two-feeder dynamic voltage restorer for application in custom power parks," *Energies*, vol. 12, no. 17, p. 3248, 2019, https://doi.org/10.3390/en12173248.

[24] A. M. Ewais, A. M. Elnoby, T. H. Mohamed, M. M. Mahmoud, Y. Qudaih, and A. M. Hassan, "Adaptive frequency control in smart microgrid using controlled loads supported by real-time implementation," *PLoS One*, vol. 18, no. 4, p. e0283561, 2023, https://doi.org/10.1371/journal.pone.0283561.

[25] I. E. Maysse *et al.*, "Nonlinear Observer-Based Controller Design for VSC-Based HVDC Transmission Systems Under Uncertainties," *IEEE Access*, vol. 11, pp. 124014-124030, 2023, https://doi.org/10.1109/ACCESS.2023.3330440.

[26] T. A. Naidu, S. R. Arya, R. Maurya, and V. Rajgopal, "Compensation of voltage-based power quality problems using sliding mode observer with optimised PI controller gains," *IET Generationa Transmission & Distribution*, vol. 14, no. 14, pp. 2656-2665, 2020, https://doi.org/10.1049/iet-gtd.2019.1623.

[27] A. H. Elmetwaly *et al.*, "Modeling, Simulation, and Experimental Validation of a Novel MPPT for Hybrid Renewable Sources Integrated with UPQC: An Application of Jellyfish Search Optimizer," *Sustainability*, vol. 15, no. 6, p. 5209, 2023, https://doi.org/10.3390/su15065209.

[28] W. Luo, Y. Yin, X. Shao, J. Liu, and L. Wu, "State Estimation and Control of Three-Phase Two-Level Converters via Sliding Mode," *Advanced Control Methodologies For Power Converter Systems*, vol. 413, pp. 65-80, 2022, https://doi.org/10.1007/978-3-030-94289-2_4.

[29] H. Boudjemai *et al.*, "Application of a Novel Synergetic Control for Optimal Power Extraction of a Small-Scale Wind Generation System with Variable Loads and Wind Speeds," *Symmetry*, vol. 15, no. 2, p. 369, 2023, https://doi.org/10.3390/sym15020369.

[30] C. Tu *et al.*, "Dynamic voltage restorer with an improved strategy to voltage sag compensation and energy self-recovery," *CPSS Transactions on Power Electronics and Applications*, vol. 4, no. 3, pp. 219-229, 2019, https://doi.org/10.24295/CPSSTPEA.2019.00021.

[31] N. Abas, S. Dilshad, A. Khalid, M. S. Saleem and N. Khan, "Power Quality Improvement Using Dynamic Voltage Restorer," *IEEE Access*, vol. 8, pp. 164325-164339, 2020, https://doi.org/10.1109/ACCESS.2020.3022477.

[32] E. M. Molla and C. -C. Kuo, "Voltage Sag Enhancement of Grid Connected Hybrid PV-Wind Power System Using Battery and SMES Based Dynamic Voltage Restorer," *IEEE Access*, vol. 8, pp. 130003-130013, 2020, https://doi.org/10.1109/ACCESS.2020.3009420.

[33] E. M. Molla and C. C. Kuo, "Voltage quality enhancement of grid-integrated pv system using battery-based dynamic voltage restorer," *Energies*, vol. 13, no. 21, p. 5742, 2020, https://doi.org/10.3390/en13215742.

[34] M. Awad, M. M. Mahmoud, Z. M. S. Elbarbary, L. Mohamed Ali, S. N. Fahmy, and A. I. Omar, "Design and analysis of photovoltaic/wind operations at MPPT for hydrogen production using a PEM electrolyzer: Towards innovations in green technology," *PLoS One*, vol. 18, no. 7, p. e0287772, 2023, https://doi.org/10.1371/journal.pone.0287772.

[35] H. Boudjemai *et al.*, "Experimental Analysis of a New Low Power Wind Turbine Emulator Using a DC Machine and Advanced Method for Maximum Wind Power Capture," *IEEE Access*, vol. 11, pp. 92225-92241, 2023, https://doi.org/10.1109/ACCESS.2023.3308040.

[36] B. Pattanaik, S. M. Hussain, V. Karthikeyan, and G. Giftson Samuel, "Energy Storage System with Dynamic Voltage Restorer Integrated for Wind Energy System," *Journal of Physics: Conference Series*, vol. 1964, no. 4, p. 042098, 2021, https://doi.org/10.1088/1742-6596/1964/4/042098.

[37] N. F. Ibrahim *et al.*, "A new adaptive MPPT technique using an improved INC algorithm supported by fuzzy self-tuning controller for a grid-linked photovoltaic system," *PLoS One*, vol. 18, no. 11, p. e0293613, 2023, https://doi.org/10.1371/journal.pone.0293613.

[38] T. M. Navinkumar, R. Aruljothi, M. Srinivasan, and A. A. Stonier, "Hybrid PV-Wind System With Power Quality Improvement Using PV-DVR," *IOP Conference Series: Materials Science and Engineering*, vol. 1055, no. 1, p. 012145, 2021, https://doi.org/10.1088/1757-899X/1055/1/012145.

[39] M. M. Mahmoud, "Improved current control loops in wind side converter with the support of wild horse optimizer for enhancing the dynamic performance of PMSG-based wind generation system," *International Journal of Modelling and Simulation*, vol. 43, no. 6, pp. 952-966, 2023, https://doi.org/10.1080/02286203.2022.2139128.

[40] M. M. Mahmoud, B. S. Atia, A. Y. Abdelaziz, and N. A. N. Aldin, "Dynamic Performance Assessment of PMSG and DFIG-Based WECS with the Support of Manta Ray Foraging Optimizer Considering MPPT, Pitch Control, and FRT Capability Issues," *Processes*, vol. 10, no. 12, p. 2723, 2022, https://doi.org/10.3390/pr10122723.

[41] N. F. Ibrahim *et al.*, "Multiport Converter Utility Interface with a High-Frequency Link for Interfacing Clean Energy Sources (PV\Wind\Fuel Cell) and Battery to the Power System: Application of the HHA Algorithm," *Sustainability*, vol. 15, no. 18, p. 13716, 2023, https://doi.org/10.3390/su151813716.

[42] N. A. N. Aldin, W. S. E. Abdellatif, Z. M. S. Elbarbary, A. I. Omar and M. M. Mahmoud, "Robust Speed Controller for PMSG Wind System Based on Harris Hawks Optimization via Wind Speed Estimation: A Real Case Study," *IEEE Access*, vol. 11, pp. 5929-5943, 2023, https://doi.org/10.1109/ACCESS.2023.3234996.

[43] M. M. Mahmoud *et al.*, "Integration of Wind Systems with SVC and STATCOM during Various Events

to Achieve FRT Capability and Voltage Stability: Towards the Reliability of Modern Power Systems," *International Journal of Energy Research*, vol. 2023, no. 1, pp. 1-28, 2023, https://doi.org/10.1155/2023/8738460.

[44] E. Mattos, A. M. S. S. Andrade, G. V. Hollweg, J. Renes Pinheiro and M. Lucio da Silva Martins, "A Review of Boost Converter Analysis and Design in Aerospace Applications," *IEEE Latin America Transactions*, vol. 16, no. 2, pp. 305-313, 2018, https://doi.org/10.1109/TLA.2018.8327380.

[45] M. M. Mahmoud, M. K. Ratib, M. M. Aly, and A. M. M. Abdel–Rahim, "Application of Whale Optimization Technique for Evaluating the Performance of Wind-Driven PMSG Under Harsh Operating Events," *Process Integration and Optimization for Sustainability*, vol. 6, pp. 447-470, 2022, https://doi.org/10.1007/s41660-022-00224-8.

[46] V. K. Goyal and A. Shukla, "Isolated DC–DC Boost Converter for Wide Input Voltage Range and Wide Load Range Applications," *IEEE Transactions on Industrial Electronics*, vol. 68, no. 10, pp. 9527-9539, 2021, https://doi.org/10.1109/TIE.2020.3029479.

[47] B. S. Atia *et al.*, "Applications of Kepler Algorithm-Based Controller for DC Chopper: Towards Stabilizing Wind Driven PMSGs under Nonstandard Voltages," *Sustainability*, vol. 16, no. 7, p. 2952, 2024, https://doi.org/10.3390/su16072952.

[48] S. R. K. Joga *et al.*, "Applications of tunable-Q factor wavelet transform and AdaBoost classier for identification of high impedance faults: Towards the reliability of electrical distribution systems," *Energy Exploration & Exploitation*, 2024, https://doi.org/10.1177/01445987241260949.

[49] Z. Du, F. Yufan, X. Yang and J. Li, "Design of PI Controller for a Class of Discrete Cascade Control Systems," *IEEE Transactions on Automation Science and Engineering*, vol. 20, no. 4, pp. 2607-2615, 2023, https://doi.org/10.1109/TASE.2022.3204531

[50] M. I. Mosaad, M. O. Abed El-Raouf, M. A. Al-Ahmar, and F. M. Bendary, "Optimal PI controller of DVR to enhance the performance of hybrid power system feeding a remote area in Egypt," *Sustainable Cities and Society*, vol. 47, p. 101469, 2019, https://doi.org/10.1016/j.scs.2019.101469.

[51] A. Ganguly, P. K. Biswas, C. Sain, A. T. Azar, A. R. Mahlous, and S. Ahmed, "Horse Herd Optimized Intelligent Controller for Sustainable PV Interface Grid-Connected System: A Qualitative Approach," *Sustainability*, vol. 15, no. 14, p. 11160, 2023, https://doi.org/10.3390/su151411160.

[52] R. S. Pal and V. Mukherjee, "Student psychology and social group optimizations based modified synchronous reference frame control topology for PV-DSTATCOM," *Electric Power Systems Research*, vol. 213, p. 108677, 2022, https://doi.org/10.1016/j.epsr.2022.108677.

[53] A. M. Ewias *et al.*, "Advanced load frequency control of microgrid using a bat algorithm supported by a balloon effect identifier in the presence of photovoltaic power source," *PLoS One*, vol. 18, no. 10, p. e0293246, 2023, https://doi.org/10.1371/journal.pone.0293246.